UNIVERSITY OF UDINE

PhD in Biomedical Science and Biotechnology
XXVII cycle

PhD Thesis

"Metabolic alterations and mitochondrial bioenergetic profile in HDAC4-driven tumorigenesis"

PhD Student:
Dr. Paolo Peruzzo

Supervisors:
Prof. Irene Mavelli
Prof. Claudio Brancolini

Academic Year 2014 - 2015

INDEX

INTRODUCTION

HDACs – a heterogeneous family of transcriptional repressors

How the cells adapt to a constantly challenging environment is one of the most studied topic of the biological science and, despite a growing body of experimental data, a comprehensive scenario is still missing. In general, cells face a particular stimulus by activating a complex response that ultimately leads to a change in the gene expression profile. In a specific moment, the chromatin status of a gene determines its propensity to be actively transcribed and two main classes of epigenetic modifiers are able to switch the chromatin organization from a condensed to a relaxed conformation – the Histone Acetyltransferases (HATs) – or viceversa – the Histone Deacetylases (HDACs). By acetylating the lysine's ε-amino group of the histone tails, HATs decrease the overall positive charge of histones leading to a decrease in their interaction with the negatively charged DNA and, thus, allowing the transcriptional machinery to access the gene locus. In contrast, the deacetylation of histones by HDACs increases their affinity for DNA, tightening the chromatin and reducing the transcriptional activity (Narlikar GJ *et al.*, 2002). Hyperacetylation of lysine residues in the N-terminus of core histones, indeed, is commonly found in promoter and enhancer sequences, as well as in intragenic regions of actively transcribed genes, demonstrating the key role of this post-translational modification in the initiation and elongation phases of the transcription process. Conversely, HDACs have been traditionally associated with gene repression and a great body of evidences supports this notion. Interestingly, recent finding coming from whole-genome mapping and ChIP-seq experiments revealed that the majority of HDACs in the human genome are associated also with active genes, suggesting the possibility that the main function of HDACs is to remove the acetyl group added by HATs and to reset the "histone code" following gene activation (Wang Z *et al.*, 2009). In addition, the deacetylation of non-histone proteins, such as several transcription factors can result in either their activation or inactivation and hence impacting the expression of their target genes.

In the human genome 18 proteins which contain a deacetylase domain exist. The deacetylases have been classified into two main macrogroups according to their homology with the yeast orthologues and to their co-factor dependence. The first

group, to which all the HDACs that need a zinc ion for their catalytic activity belong, is further divided into 4 classes: class I (HDAC1, 2, 3, 8); class IIa (HDAC4, 5, 7, 9); class IIb (HDAC6, 10) and class IV (HDAC11). The second group, instead, is composed by deacetylases which require NAD^+ as co-factor and, since homologous to budding yeast Sir2, are commonly designed as Sirtuins (SIRT1-7). Ubiquitously expressed and with a subcellular localization that is completely nuclear, class I HDACs are thought to be the "canonical" histone deacetylases and share sequence similarity with budding yeast Rpd3. Structurally, they are constituted by a central deacetylase domain with very small N- and C-termini. With the exception of HDAC8, all class I HDACs work in multiprotein repressor complex, such as NuRD, sin3, CoREST, NcoR or SMRT, whose subunits can activate the catalytic domain of HDACs and conjugate coherent functions (ATP-dependent nucleosome-remodeling, histone demethylation) for initiation and/or maintenance of gene silencing. Recently, the crystal structure of HDAC3 in complex with its co-repressor SMRT was solved and it was demonstrated that HDAC3 binding to a D-myo-inositol-1,4,5,6-tetrakisphosphate is essential for complex formation acting as an "intramolecular glue" (Watson PJ *et al.*, 2012). HDAC8, which not requires assembly into multiprotein complexes for its fully activation, displays important structural differences, exactly in the corresponding region of HDAC3-SMRT-inositol interaction. This structural peculiarity allows a better access of the substrate to the active site of HDAC8 compared to the naive HDAC3 (**figure 1A**).

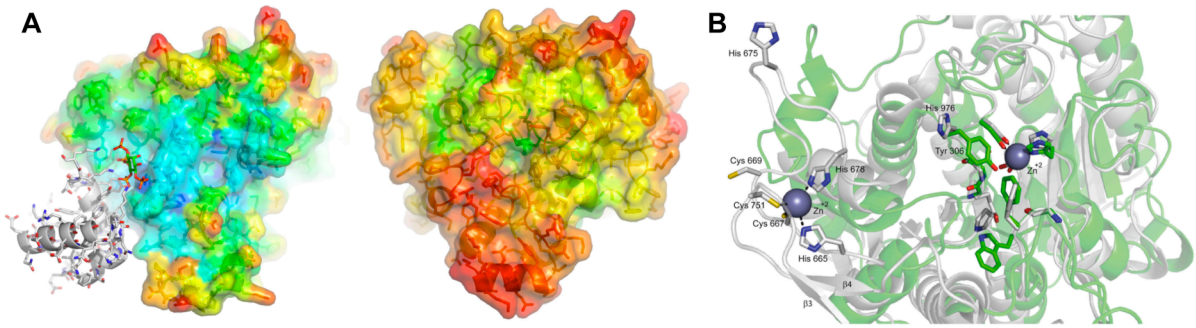

Figure 1: **Crystal structures of representative class I and IIa HDACs. A)** Surface representations of class I HDAC3 complexed with the deacetylase activation domain (DAD) of SMRT/Ncor2 (left) and HDAC8 (right), coloured by crystallographic temperature factors (blue to red = low to high). HDAC8's surface around the active site is relatively disordered, yet the catalytic site is accessible. **B)** Superimpositiion of the inhibitor (TFMK)-bound ribbon structure of HDAC8 (*in green*) and of HDAC4 (*in white*) catalytic sites. Note that His 976 in HDAC4 is rotated away from the active site differently from Tyr 306 in HDAC8. The His/Tyr substitution in HDAC4 prevents the formation of the hydrophilic tunnel necessary for the release of the reaction product (adapted from Watson PJ *et al.*, 2012 and from Di Giorgio E *et al.*, 2014).

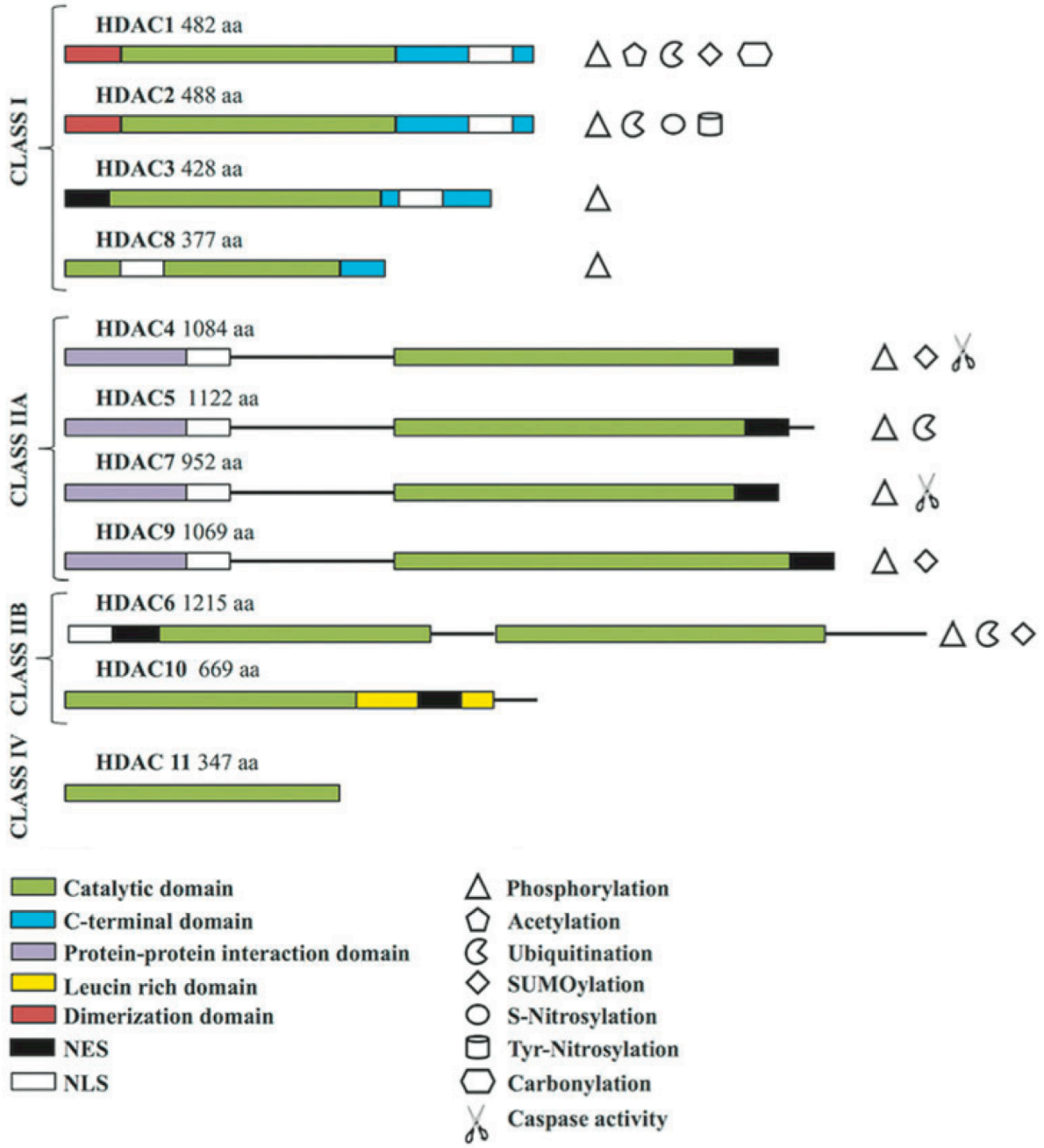

Figure 2: **Schematic representation of human zinc-dependent histone deacetylases.** All zinc-dependent HDACs present a modular organization with a highly conserved catalytic domain (*in green*). Apart from HDAC10 and HDAC11, all HDACs possess a nuclear localization signal (NLS, *in white*) and, along with HDAC3, all class II HDACs are characterized by a nuclear export signal (NES, *in black*). For each human HDAC, the amino acids' protein length and the known post-translational modifications are reported (adapted from Chiaradonna F *et al.*, 2014).

HDAC4 and class IIa HDACs

Class IIa HDACs, and more in general class II HDACs, are defined by their phylogenetic similarity to budding yeast Hda1. Their bipartite structure is characterized by a conserved C-terminal deacetylase domain and a long N-terminal adaptor region that is mainly devoted to protein-protein interactions and site of post-translational modifications that regulate class IIa HDAC subcellular localization and functions.

Despite class I and class IIa HDACs share a very similar deacetylase domain, class IIa display a neglected deacetylase activity which is about 1000 fold less compared to class I HDACs. The low enzymatic activity toward acetyl-lysines of class IIa HDACs is caused by an aminoacid substitution (Tyr 976 His in HDAC4) in the catalytic pocket that is conserved in all vertebrate class II HDACs (**figure 1B**). Thanks to crystallographic analysis, it was determined that, while in class I and IIb HDACs the hydroxyl group of the tyrosine^{306} can stabilize the transition state of the reaction, by hydrogen bonding with the oxyanion intermediate, the corresponding histidine^{976} side chain in HDAC4 is pointing outward the catalytic site, thus limiting its stabilizing power toward the intermediate and selecting for a low enzymatic activity (Bottomley MJ *et al.*, 2008). Notably, the gain of function mutant H976Y of HDAC4 in which the histidine is restored to tyrosine shows a deacetylating capability that is 1000 fold higher than HDAC4^{WT} (Lahm A *et al.*, 2007), confirming the importance of this mutational event in the evolution of class IIa HDACs. Nevertheless, a deacetylase activity can be associated with class IIa HDACs *in vivo* since the catalytic domain of HDAC4 is able to physically interact with the NCoR co-repressor via its repression domain 3 (RD3) in a multiprotein complex in which the deacetylase activity is granted by class I HDAC3 (Fischle W *et al.*, 2002).

The long N-terminal region characterizes the class IIa HDACs (**figure 2**). This region contains a nuclear localization signal (Wang AH and Yang XJ, 2001) and a region devoted to the binding to several transcription factors, the most characterized being the myocyte enhancer factor 2 (MEF2) family members (Lu J *et al.*, 2000). The amino-terminal region is also responsible for the interaction with the chaperones like β- and ε-14-3-3 proteins, which play important function in the regulation of class IIa activity (Wang AH *et al.*, 2000). Since class IIa HDACs are not able to bind directly the DNA and given their ability to interact with both transcription factors and co-

repressors, the emerging model is that class IIa HDACs function as a bridging factor to tether the repressor complex to the transcription factor binding sites in the genome. However, a puzzling finding was made by Zhou and colleagues, through the identification of a splicing variant of HDAC9, which lacks exon 22 at the carboxy-terminus and so the deacetylase domain. This truncated version of the deacetylase was still able to repress the transcription of MEF2 target genes (Zhou X *et al.*, 2001). This observation was further confirmed when it was discovered that the 289 aa amino-terminal fragment of HDAC4 generated by caspase-2/3 processing during apoptosis accumulates in the nuclear compartment where it acts as a potent transcriptional repressor of MEF2 activity (Paroni G *et al.*, 2004).

Class IIa HDACs possess both nuclear localization signal (NLS) and nuclear export sequence (NES) presents at the carboxy-terminus, the N-terminal domain is also indirectly responsible for their subcellular localization. In fact, in this region a set of serine residues is conserved among all class IIa HDAC members and can be target of phosphorylation by multiple kinases. Once phosphorylated, these serines become docking site for 14-3-3 chaperon proteins, which drive class IIa HDACs out of the nucleus, thus relieving their repressive potential. In other words, the phosphorylation status of these key serines governs the nucleus-cytoplasmic shuttling of these enzymes; a distinctive feature of class IIa HDACs. In accordance, site-specific mutagenesis to substitute Ser^{246}, Ser^{467} and Ser^{632} (in HDAC4) with alanine generates a phospho-resistant mutant of HDAC4 that displays increased nuclear localization and operates as a super-repressor of MEF2-dependent transcription (Grozinger CM and Schreiber SL, 2000). Several kinases have been implicated in the regulation of class IIa HDACs subcellular localization. For instance, it has been shown that calcium/calmodulin-dependent protein kinases (CaMKs) are able to phosphorylate HDAC4 and HDAC5, although with different dynamics, resulting in their binding to 14-3-3 proteins, nuclear export and consequent disruption of the MEF2-HDAC complex. Through this mechanism CaMK signalling can affect the myogenic program under the control of MEF2 during the fibroblast-to-muscle differentiation process (McKinsey TA *et al.*, 2000). A similar mechanism was proposed in the case of HDAC4-SRF interaction in cardiac myocites challenged with a hypertrophic stimulus. In this context, calcium influx and CaMK-IV activation, through HDAC4 phosphorylation and its cytoplasmic sequestration, allow SRF to dissociate from HDAC4 and enhance SRF-dependent transcription (Davis FJ *et al.*,

2003). In summary, class IIa HDACs act as nodal regulators of striated muscle stress response by linking upstream Ca^{2+}-dependent kinases to downstream gene program involved in hypertrophy. Interestingly, in cardiomyocytes PKA, whose activity can be stimulated by short repetitive catecholaminergic pulses, exerts an opposite effect with respect to CaMKs on the MEF2-HDAC4 axis. Activated PKA is able to indirectly but reproducibly induce a proteolytic cleavage of HDAC4. This uncharacterized proteolytic activity generates a N-terminal fragment that localizes into the nucleus where it serves as MEF2 repressor. Intriguingly, this HDAC4 N-terminal fragment shows a higher repressive potential against MEF2 compared to SRF, demonstrating that PKA-dependent HDAC4 proteolysis results in differential regulation of target transcription factors (Backs J *et al.*, 2011).

Not all the phosphorylation events acting on class IIa HDACs show the invariable outcome of the cytoplasmic retention of these proteins. It has been demonstrated that in C2C12 myoblasts, the constitutive activation of MAPK signalling by oncogenic HRAS or MEK1, which culminates with the switch on of ERK1/2 kinases, results in HDAC4 nuclear accumulation. In this case, the nuclear shuttling of HDAC4 can be justified by the MEF2-dependent repression of MyoD and myogenin and the inhibition of muscular differentiation of myoblasts as operated by mitogens or by oncogenic RAS signaling (Zhou X *et al.*, 2000).

Cancer cell metabolism: a step out Warburg's shadow

It's hard to start a discussion about cancer without first mentioning the seminal review by Hanahan and Weinberg in which the hallmarks of cancer cells have been described and categorized. Those fundamental hallmarks, namely the autonomous sustained proliferative signalling, the evasion from growth suppressors control, the resistance to cell death mechanisms, the unlimited replicative potential, the induction of angiogenesis and the activated invasion and metastasis programs underlie selective advantages that cancer cells acquire via distinct mechanisms and at various times during the multistep tumorigenesis process *in-vivo* (Hanahan D and Weinberg RA, 2000). However, during the last decade, another new basic characteristic of tumor cells has been recognized and comprised among the cancer hallmarks: the metabolic reprogramming (Hanahan D and Weinberg RA, 2011). Despite a renewed interest in this field has re-emerged quite recently, the metabolic reprogramming of

cancer cells was already known since the pioneering work by Otto Warburg in 1920s. In his seminal research, he noticed that ascites tumor cells consume more glucose than normal cells and the majority of glucose-derived carbons can be retrieved in secreted lactate, even in the presence of an oxygen concentration that would allowed oxidative phosphorylation (OXPHOS) to proceed (Warburg O, 1927). These peculiar features have been observed in several types of cancers and constitute the fundamental principles of the so-called "Warburg effect". In order to justify the increased dependence from glycolysis and the concomitant decrease in respiration observed in tumor cells with respect to normal cells, it has been postulated a model in which cancer cells arise from the body of normal cells in two temporally distinct phases. In the first phase an irreversible injury of mitochondrial respiration takes place and is followed by a second phase of cancer formation where the selective pressure saves only those cells that succeed in replacing the irretrievably lost respiration energy by fermentation (Warburg O, 1956). Therefore, from a biological point of view, this altered metabolism confers to cancer cells a selective advantage for survival and proliferation in the unique tumor microenvironment characterized by continuously fluctuating oxygen levels (Hsu PP and Sabatini DM, 2008). However, this implies that, just to meet the energy demand for sustained cell proliferation and given that glycolysis is 18 times less efficient in terms of ATP production per glucose molecule compared to mitochondrial oxidative phosphorylation, cancer cells need to up-regulate the glucose flux through glycolysis several times. While this is true for most human tumors for the radiological visualization of which ^{18}FDG-PET is clinically employed by virtue of their pronounced avidity for this glucose analogue, the issue regarding the presence of a real mitochondrial defect that can account for a "compensatory" increase in *aerobic* glycolysis is still debated in the scientific community. In most cancer cells, mitochondria are not defective for the capability of carrying out oxidative phosphorylation, but they are actually reprogrammed to meet the augmented biosynthetic needs that a cancer cell experiences (Ward PS and Thompson CB, 2012). Cell proliferation, indeed, is a costly process not only in terms of ATP consumption but also because it involves the *de-novo* synthesis of cellular components like nucleotides, fatty acids and membrane lipids for cell duplication. Under this view, the increased glycolysis flux can foster the production of various glycolytic intermediates that can be diverted to other biosynthetic pathways such as, for example, the pentose phosphate pathway (PPP). Hexokinase is the enzyme

responsible for the conversion of glucose to glucose-6-phosphate (G6P) and is frequently upregulated in various tumor cell lines, among which cervix carcinoma HeLa and AS-30D hepatoma cells could be cited. G6P, as a substrate for the first rate-limiting enzyme of the PPP – the glucose-6-phosphate dehydrogenase (G6PD) –, can feed the oxidative arm of the pathway in order to generate NADPH, the principal intracellular reducing molecule required for the biosynthesis of lipids, and ribose-5-phosphate, an essential precursor for nucleotides biosynthesis. Furthermore, glycolysis can provide dihydroxyacetone phosphate for triacylglyceride and phospholipid synthesis, 3-phosphoglycerate for serine, cysteine and glycine synthesis and pyruvate for oxidative phosphorylation and for alanine and malate synthesis. So the rationale for cancer cells of upregulating the glucose flux through glycolysis is to maximize the activity of lower-flux biosynthetic pathways, even though this results in a high rate of lactate production (DeBerardinis RJ *et al.*, 2008). From this perspective, it is not surprising that most cancer cell lines, including A549 and H1299 lung carcinoma, 293T transformed embryonic kidney and HeLa cervix carcinoma cell lines, express the embryonic M2 splice variant isoform of pyruvate kinase (PK), the enzyme that catalyzes the third irreversible reaction of glycolysis by transforming phosphoenolpyruvate into pyruvate. The PKM2 is a less efficient isoform compared to PKM1 (the one expressed by normal adult cells), thus acting as a bottleneck of the pathway causing the upstream intermediates to accumulate and to be available for the biosynthetic pathways (Christofk HR *et al.*, 2008). Moreover, cancer cells can also take advantage from mitochondrial tricarboxylic acid (TCA) cycle intermediates for biosynthetic reactions. The classic example is the continuous efflux (cataplerosis) of citrate from the mitochondria to the cytoplasm, where, thanks to the catalytic activity of ATP citrate lyase, an enzyme often upregulated in tumor cells (Gao Y *et al.*, 2014), can be converted to oxaloacetate and acetyl-CoA. Cytoplamic acetyl-CoA, beyond being the source of acetyl groups for HATs, is used by fatty acid synthase, another enzyme frequently overexpressed in human tumors (Menendez JA *et al.*, 2007), to generate lipids and cholesterol, while oxaloacetate is transformed by malate dehydrogenase to malate which, in turn, can either return to the mitochondria or be converted to pyruvate by malic enzyme and contribute to lactate production (Icard P *et al.*, 2012). This example demonstrates that TCA-functional mitochondria not only are present and active in cancer cells but they are also necessary to sustain tumor growth. The importance of a functional mitochondrial

compartment for cancer proliferation is confirmed by the glutamine addiction that many cancer cells display. In fact, in order to replenish the loss of TCA intermediates, because of citrate efflux from mitochondria, cancer cells engage in an anaplerotic mechanism that involves the glutamine-derived glutamate conversion into α-ketoglutarate (Hensley CT *et al.*, 2013). In this way, the glutaminolysis can serve the double purpose of generating reducing equivalents for the mitochondrial electron transport chain and to provide the cell, through the cytosolic conversion of glutamine-derived malate to pyruvate, with the essential NADPH for fuelling fatty acid synthesis, as in the case of glycolytic SF188 human glioblastoma cell line (DeBerardinis RJ *et al.*, 2007). In the same cell line, which was originally isolated from a patient whose tumor displayed an amplification of c-Myc, the mitochondrial glutamine metabolism is under the control of Myc. This oncogene/transcription factor can associate to the promoter of the high affinity glutamine importers, ASCT2 and SN2, upregulating their expression levels (Wise DR *et al.*, 2008). Further supporting the importance of glutaminolysis for cancer cell proliferation, recently it has been shown that murine fibroblast NIH-3T3 cells overexpressing an hyperactive form of K-Ras, once deprived of glutamine, display an abortive S-phase (Gaglio D *et al.*, 2009) and the anaplerotic block of glutamine utilization in cancer cells harboring K-Ras mutations causes S or G2/M cell cycle arrest and sensitizes cells to cytotoxic drug treatments (Saqcena M *et al.*, 2014). Interestingly, it was discovered that glutamine-supported oxidative phosphorylation is a major source of ATP, both in normoxic and hypoxic conditions, in 4T1 Akt-driven mouse mammary tumor cell line, in ASPC1 K-Ras-driven human pancreatic cancer cell line, as well as in iBMK murine renal epithelial cells constitutively overexpressing either oncogenic H-Ras^{G12V} or myristoylated Akt, both proteins known to induce the Warburg phenotype. Notably, however, the inhibition of OXPHOS has a higher impact in terms of ATP/ADP ratio in Akt- compared to Ras-overexpressing cells, underlining the heterogeneity which characterizes the metabolic regulation in cancer cells, especially regarding oxidative phosphorylation control (Fan J *et al.*, 2013). In a computational analysis performed by Hu and collegues on 1421 human genes classified as “metabolic” according to KEGG database, in more than 2500 microarray gene expression profiles spanning 22 different tumor types, it has been demonstrated that, if the glycolysis and the purine/pyrimidine biosynthetic pathway are commonly up-regulated in many tumors, this is not the case for oxidative phosphorylation. As a matter of fact, OXPHOS genes

has the most heterogeneous expression pattern among the considered cancer types, being significantly down-regulated in brain, colon, kidney, pancreatic and thyroid cancers whereas consistently up-regulated in breast, leukemia, lung, lymphoma and ovarian cancers (Hu J *et al.*, 2013). This scenario is getting even more complicated if we consider that the OXPHOS gene expression profile is not only heterogeneous between different tumor types but also between samples of the same tumor, suggesting that the activity of oxidative phosphorylation is influenced by both the environmental variability across different tumors and the specific physiological conditions and/or genetic background of individual tumors in each patient (Hu J *et al.*, 2013). Therefore, although most tumor cell types show an enhanced glycolytic flux, not all have a diminished mitochondrial metabolic capacity. In other words, the accelerated cellular proliferation may impose an energy deficiency that, together with a higher demand for glycolytic and TCA cycle intermediates for biosynthetic purposes, can be satisfied only by increasing the glycolytic flux leaving, in the meanwhile, the oxidative phosphorylation unperturbed (Moreno-Sánchez R *et al.*, 2007).

One of the six founder hallmarks of cancer described by Hanahan and Weinberg is the independence from growth signalling for proliferation. Normal cells, do not proliferate autonomously and enter and progress through the cell cycle only when systemic growth factors are present in the environment and capable of interaction with the relative receptors. This engagement turns on molecular pathways that ultimately activate gene programs leading to cell proliferation. Interestingly, in the absence of an appropriate growth stimulus, normal cells rapidly lose the membrane transporters of nutrient – mainly glucose and glutamine – and, just to retrieve the ATP support necessary for survival, engage the autophagy process (Thompson CB *et al.*, 2005). In cancer cells the proliferation-promoting pathways downstream the growth factors signalling are often constitutively engaged because of the oncogene activation, which confers the well-known independence from environmental growth signals. An important effect of the constitutive activation of these pathways is the enhancement of nutrient uptake from the environment, thanks to the overexpression of the relative membrane importers. This strategy allows cancer cells to generate the high glycolytic and glutaminolytic fluxes, which are needed to maintain a metabolic phenotype of biosynthesis, independently from normal physiologic constraints, rendering cancer cells a metabolic-autonomous entity (DeBerardinis RJ *et al.*, 2008).

Therefore, cellular metabolism and oncogene activation (or tumor suppressor inactivation) are two faces of the same coin, being intimately cross-linked and under the reciprocal influence. Hence, not surprisingly, the key components of the Warburg effect, namely the increased glucose consumption and aerobic glycolysis (with or without a decrease in the oxidative phosphorylation) accompanied by the concomitant increase in lactate secretion, are also distinguishing features of oncogene activation (**figure 3**).

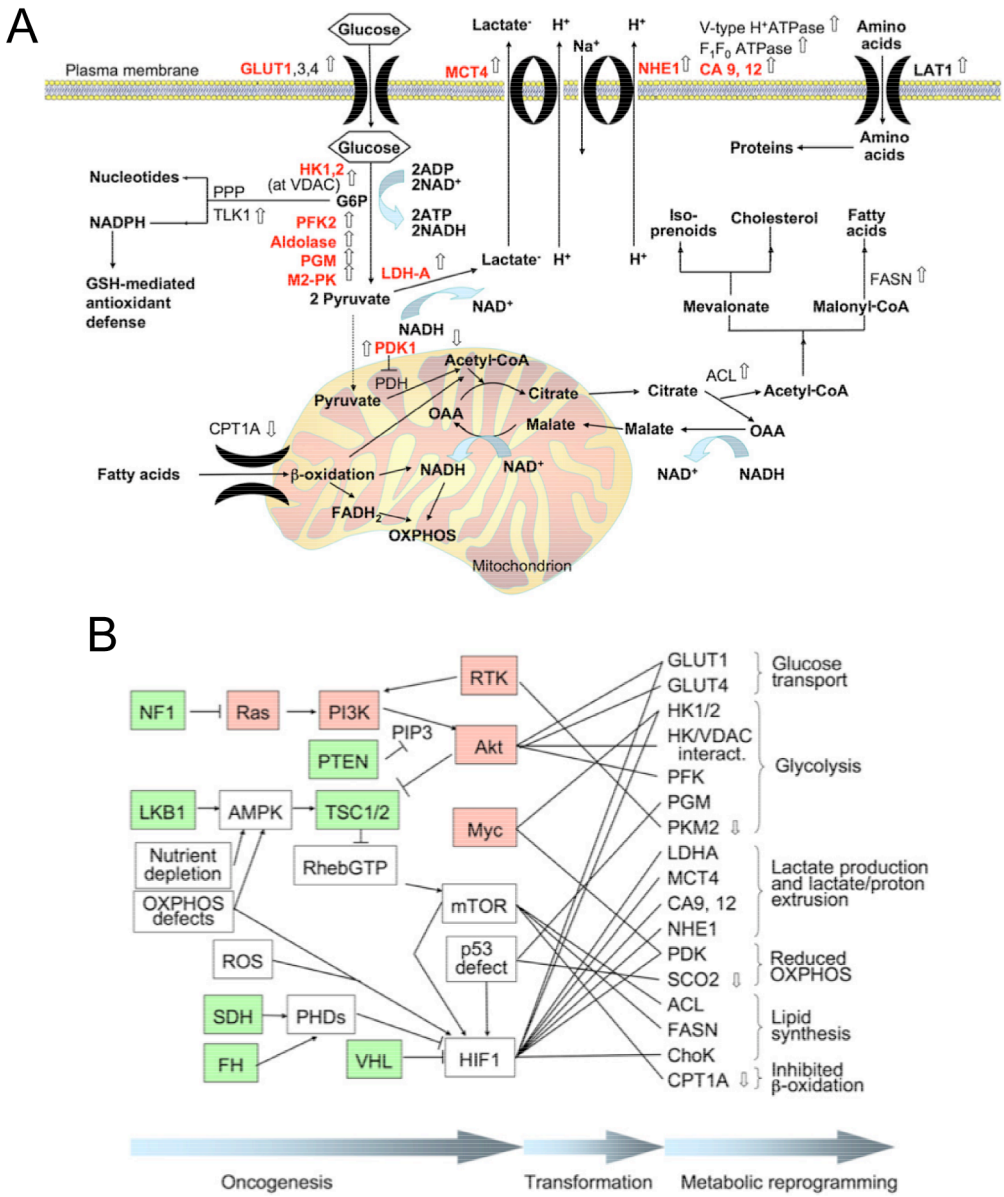

Figure 3: **Metabolic reprogramming of cancer cells. A)** In normal cells, the imported glucose is metabolized to pyruvate which is converted to acetyl-CoA and completely oxidized, through the mitochondrion-localized TCA cycle, to CO_2 and H_2O. In contrast, the aerobic glycolysis in tumor cells implies the conversion of glucose to pyruvate and subsequently into the waste product lactate. Moreover, in cancer cells, acetyl-CoA tends to be introduced into a truncated TCA cycle from which the citrate is exported to the cytosol to

be converted again in acetyl-CoA and serves as a building block for cell growth and proliferation. **B)** As a result of oncogenes gain of functions (*in pink*) or the the loss of function of tumor suppressor genes (*in green*) affecting the Ras pathway or the PI3K/Akt/mTOR/HIF pathway, the typical pattern of metabolic changes is induced, leading to cancer-associated alterations in basal metabolism (adapted from Kroemer G & Pouyssegur J, 2008).

Oncogenes' metabolic face

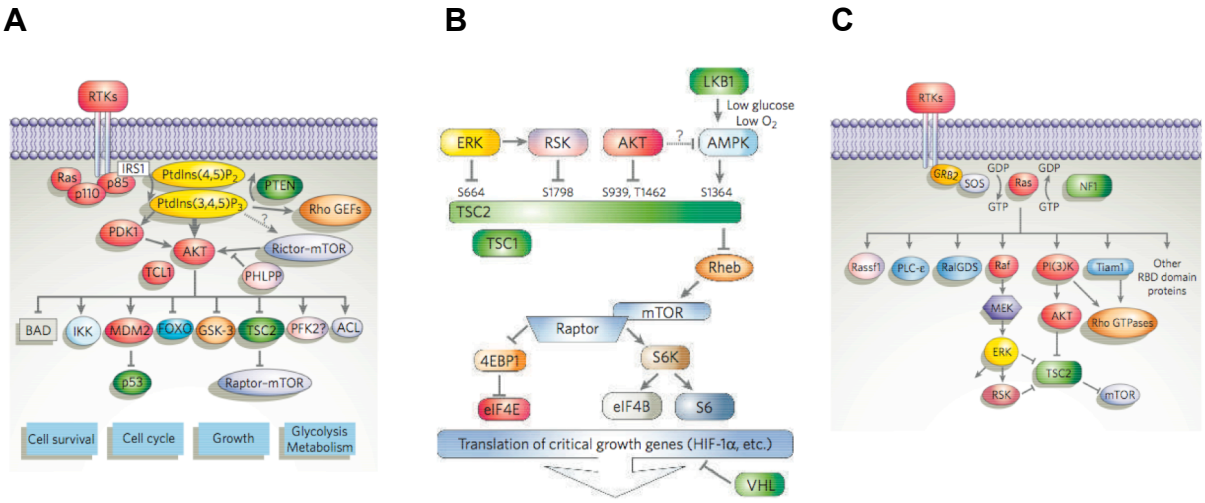

Figure 4: **Representation of main oncogene signalling molecular pathways. A)** The PI3K signalling: class IA PI3Ks are heterodimers of p85 regulatory subunit and p110 catalytic subunit and are capable to phosphorylate phosphatidylinositol-4,5-bisphosphate generating the membrane-bound second messenger phosphatidylinositol-3,4,5-triphosphate which is recognized by a set of signalling proteins with pleckstrin homology domain, the most characterized of which is the serine/threonine kinase Akt. Akt controls cell survival, cell cycle, cell growth and metabolism through phosphorylation of a pletora of key substrates. **B)** the mTOR signalling: mTOR kinase is an integrator of growth factor and nutrients signals. Growth factor signalling through Ras-Erk and PI3K-Akt axes activates mTORC1, while low nutrient availability or hypoxia inhibit mTORC1, in part through the LKB1-AMPK pathway. **C)** The Ras signalling: upon growth factors binding, receptor tyrosine kinase (RTK) dimerizes leading to phosphorylation of their tyrosines in the cytoplasmic face. These phospho-tyrosines become docking sites for adaptor proteins such as GRB2 and GEF like SOS that can activate Ras GTPases. Upon activation, Ras proteins can switch on signalling cascades that ultimately lead to cell growth and cell cycle entry. Proteins whose genes are mutationally activated in human cancers are shown in red; those inactivated are in green. (adapted from Shaw RJ & Cantley LC, 2006).

The PI3K/Akt/mTOR pathway (**figure 4A**), which is engaged by normal cells in response to a wide range of growth and also hypertrophic stimuli, represents one of the most frequently dysregulated pathway in human malignancies. The activation of the PI3K following growth-factor stimulation results in the phosphorylation of phosphatidylinositol lipids at the plasma membrane and subsequent recruitment and phosphorylation-dependent activation of the serine/threonine kinase Akt (PKB). Beyond being amplified in certain tumors, Akt is a common downstream effector hub for multiple oncogenic pathways and its uncontrolled activity promotes the

constitutive expression of cell-surface nutrient receptors, as well as the upregulation of proliferation-related macromolecules biosynthesis, such as lipids and, through the mTOR activity, proteins. On the other hand, Akt activation is sufficient to induce the Warburg phenotype in leukemia and glioblastoma cell lines causing a dose-dependent stimulation of aerobic glycolysis that results in increased lactate secretion, without affecting oxygen consumption. In accordance, PI3K inhibition in these cell lines blunts the glucose uptake and lactate production (Elstrom RL *et al.*, 2004). A major negative regulator of the PI3K/Akt/mTOR pathway is the phosphatase and tensin homologue deleted in chromosome ten (PTEN). This enzyme is able to switch off the signalling throughout this pathway by dephosphorylating the phosphatidylinositol-3-phosphate species, thus avoiding Akt activation. Thanks to its role in the control of the PI3K/Akt axis, PTEN is considered as an oncosuppressor and loss of PTEN is a common genetic lesions observed in several human tumor types, including breast, ovarian, colon cancers and glioblastomas. Interestingly, the systemic overexpression of PTEN in mice results in smaller animals (because of lower organ cellularity), confirming the anti-proliferative function of this protein, but, more importantly, determines a tumor suppressive metabolic state characterized by decreased glucose consumption and lactate extrusion accompanied by increased mitochondrial oxygen consumption and ATP production as well as mitochondrial biogenesis. Mechanistically, the overexpression of PTEN *in-vivo* redirects, thanks to the decreased PKM2 protein levels, a great fraction of glycolytic intermediates into oxidative phosphorylation at the expense of lipid biosynthetic pathways, consistent with a reduced body fat accumulation in the “Super-PTEN” animals compared to normal littermates (Garcia-Cao I *et al.*, 2012). Accordingly, in a model of thyroid neoplasia progression, the thyroid-specific deletion of PTEN in mice causes the repression of TCA cycle and OXPHOS genes that influences the overall mitochondrial functionality. Surprisingly, the compensatory aerobic glycolysis observed in this transformation model is not the outcome of the increased expression of transcription factors commonly responsible for the upregulation of glycolytic gene expression, such as Myc or HIF1α. Instead, it relies on the PI3K/Akt-dependent inhibition of the AMP-activated protein kinase (AMPK). Re-stimulation of AMPK, through the use of the AMP-analogue AICAR is able to reduce, at least in part, the mitochondrial defects, to reverse the glycolytic switch and, more importantly, to mitigate the thyroid hyperplasia caused by constitutive PI3K/Akt activation (Antico

Auciuch VG *et al.*, 2013). In the same direction goes the discovery that, in colon cancer cells, the miRNA-mediated downregulation of PTEN induces a similar metabolic shift (Wei Z *et al.*, 2014).

The serine/threonine kinase mechanistic target of rapamycin (mTOR) is a conserved integrator of mitogenic and nutrient stimulations in mammalian cells (**figure 4B**) and, as such, deregulated mTOR signalling is frequently observed as an underlying driving force in cancer development (Shaw RJ & Cantley LC, 2006). mTOR can be engaged into two different complexes, mTORC1 and mTORC2, whose composition in terms of ancillary proteins dictates their functional specificity and their set of downstream effectors. Although there are other proteins specifically associated with either complexes, traditionally Raptor and Rictor scaffold proteins define mTORC1 and mTORC2, respectively. mTORC1, which is the sole complex that can be effectively inhibited by rapamycin, responds to four major, not always synergistic, regulatory inputs: nutrients, growth factors, energy status and stress cues. Amino acids stimulation causes the shuttling of mTORC1, mediated by the activation of the small-GTPase Rag, to the endomembrane system (endosomes and lysosomes) where it can interact with and be activated by another small GTPase called Rheb, which in turn is stimulated by growth factors. Only when both nutrients (amino acids) and mitogenic (growth factors) stimuli are provided to the cells, mTORC1 is activated, thus operating as converging hub to generate coherent signalling in response to physiological favourable environmental conditions or to pathological hyperactivation of pro-growth pathways (Zoncu R *et al.*, 2011). Upon activation, mTORC1 is able to promote protein synthesis with two different strategies. First it phosphorylates 4E-BP1, a repressor of mRNA translation, preventing it to bind to eIF-4E and thus allowing the recruitment of the translational machinery to the 5' end of most mRNA. Second, it can favour the initiation and elongation phases of the translation process by phosphorylating and activating S6K, a key positive regulator of translation (Ma XM & Blenis J, 2009). Thanks to their functional role as GAP for Rheb, hamartin (TSC1) and tuberin (TSC2), the protein subunits of Tuberous Sclerosis Complex (TSC), are actually effective in the shutting off of mTORC1 signalling and their homozygous deletion in mice is embryonic lethal. Interestingly, however, in immortalized MEFs derived from mouse embryos lacking TSC1, an increase in glucose consumption and lactate production was observed as the result of a mTORC1-dependent increase in several glycolytic enzymes expression, expecially PKM2. The upregulation of PKM2

is achieved through two independent mechanisms: the first involves the mTORC1-HIF1α axis and implies a direct transcriptional activation of the PKM promoter by HIF1α. The second depends on the mTORC1-dependent upregulation of c-Myc that, in turn, can enhance the expression of three hnRNPs (PTB, hnRNPA1 and hnRNPA2) responsible for the repression of the alternative splicing of PKM1. This scenario applies also to human pancreatic (PANC-1) and hepatic (HepG2) cancer cell lines. The simultaneous inhibition of mTORC1 and glycolysis, or the stable knock-down of PKM2 in PC3 prostate cancer cell line, significantly retarded the development of tumors, when cancer cells were xenografted in mice (Sun Q *et al.*, 2011). Strikingly, the glycolytic switch caused by mTORC1 hyperactivation and mediated by HIF1α seems to contribute also to the sustaining of the trained immunity, the physiological ability of the innate immunity to mount an adaptive response (Cheng SC *et al.*, 2014). Therefore, mTORC1 fulfils a key role in glucose metabolism and in the induction of aerobic glycolysis, not only in malignant cells but also in proliferating normal cells. However, it has been shown that, in proliferating cells, chemical inhibition of mTORC1 impacts also mitochondrial oxidative phosphorylation by imposing a 4E-BP-dependent block in the translation of a specific subset of mitochondrial nuclear-encoded genes, among which the ATP synthase subunits ATP5D, ATP5O, ATP5G1 and ATP5L and the mitochondrial transcription factor TFAM. Accordingly, mTORC1 inhibition results in a decreased overall oxygen consumption and mitochondrial mass, but also in a consistent drop in intracellular ATP levels (Morita M *et al.*, 2013). These findings demonstrate that mTOR is not only a master regulator and inducer of glycolysis, but more in general, can act at multiple levels to coordinate the cellular increase in metabolic fluxes during high aminoacids and growth factors environmental conditions.

Oncogenic transformation driven by the Ras family of small GTPase is another signalling cascade that has been identified to alter cellular metabolism (Chiaradonna F *et al.*, 2006) (**figure 4C**). In the work of Schreiber group, the BJ human fibroblast cell line was subsequently engineered to express the catalytic domain of human telomerase, the large T antigen, the small T antigen and the oncogenic allele H-RAS to obtain a multistep progression toward full transformation. By challenging the resulting cell lines with small molecules able to modulate the aerobic as well as the anaerobic metabolism (oligomycin, 2-deoxyglucose, oxamic acid, wortmannin and rapamycin), they found that, when the cells are fully transformed by hyperactive H-

RAS, they are also more sensitive to glycolysis and lactate production inhibition, as predicted by the Warburg effect, both in terms of growth inhibition and ATP generation (Ramanathan A *et al.*, 2005). A mitochondrial dysfunction has been elucidated as a potential cause for Ras-driven aerobic glycolysis. In HEK-293T cells expressing a doxycycline-inducible oncogenic K-RAS isoform, it has been shown that, as early as 16 hours after the induction of K-RAS, mitochondrial morphology alterations such as disturbed cristae or disorganized network were already evident (Hu Y *et al.*, 2012). Furthermore, K-RAS induction determined a substantial decrease in oxygen consumption that was caused by the down-regulation of OXPHOS complex I, both in terms of protein levels and activity (Baracca A *et al.*, 2010).

The metabolic side of class IIa HDACs

It is well established that a good fraction of pivotal metabolic enzymes are subjected to reversible acetylation/deacetylation processes able to fine tune their activity or protein stability (Huang W *et al.*, 2014; Lv L *et al.*, 2011). Moreover, most pathways (both anabolic and catabolic) converge on two key molecules, acetyl-CoA and NAD^+, that are substrate or cofactor for HATs and of a particular class of HDACs – the Sirtuins –, respectively. These evidences have encouraged to hypothesize that HDACs can regulate cellular metabolism and that changes in the metabolic profile of a cell can influence the HAT/HDAC dynamic equilibrium, as a feedback loop. Thanks to their ability to shuttle between the nucleus and the cytoplasm depending on the phosphorylation status of their key serine residues, class IIa HDACs represent ideal effectors to solve a regulatory function on cytoplasmic metabolic enzymes and link metabolic changes with coherent transcriptional responses in the nucleus. In the last years several studies were published in support of this hypothesis establishing a functional link between class IIa HDACs and some metabolic responsive kinases. For instance, it has been discovered that AMP-activated protein kinase (AMPK) can phosphorylate HDAC5, promoting its nuclear export after interaction with 14-3-3 proteins. Treatment of human primary myotubes with the AMP analogue AICAR, an inducer of AMPK activity, results in the enhanced expression of glucose transporter GLUT4 following HDAC5 phosphorylation and subsequent nuclear export, which is critical for relieving the repression operated on MEF2 TFs (McGee SL *et al.*, 2008). A similar mechanism is acting also during the adaptation of skeletal muscle to exercise.

In this context, the increased contractile load that muscle cells experience during exercise causes the cytosolic Ca^{2+} concentration to increase. In this condition, CaMKII is activated by the Ca^{2+}/calmodulin complex and phosphorylates HDAC5, which dissociates from MEF2s at the promoter region of the GLUT4 gene. This phosphorylation up-regulates GLUT4 expression, in order to meet the metabolic demand of the cell during training (Ojuka EO et al., 2012). AMPK is a serine/threonine kinase belonging to the LKB1-activated kinase macrofamily, fundamental in sensing the variation in AMP/ATP ratio (and to a lesser extent the ADP/ATP ratio). For this reason, AMPK is a sensor of the bioenergetic status of the cell. In general, if an energy deficit is detected, AMPK operates to restore the energy homeostasis by promoting the engagement of pathways that generate ATP while switching off those that consume it (Hardie DG, 2014). Interestingly, in liver and hepatoma cell lines, LKB1 deletion causes the loss of basal HDAC4/5/7 phosphorylation. Conversely, the use of metformin, a widely used anti-diabetic drug for its ability to stimulate AMPK activity in an LKB1-dependent manner, leads to an increase in HDAC4/5/7 phosphorylation. More importantly, in these cell lines, class IIa HDACs subcellular localization is subjected to hormonal control: the fasting hormone glucagon or the cAMP inducer forskolin trigger a fast dephosphorylation and accumulation into the nucleus of HDAC4/5, where they are essential to promote the expression of rate-limiting enzymes belonging to gluconeogenic or glycogenolytic pathways such as the catalytic subunit of G6Pase, PEPCK and FBP1. In this context, the emerging model predicts that, following a glucagon stimulus, the increase in cyclic AMP can activate PKA that, in turn, is able to phosphorylate and inactivate AMPK. Inactive AMPK is no more prone to phosphorylate class IIa HDACs that are free to shuttle into the nucleus where they associate with the deacetylating complex composed by HDAC3/NCOR/SMRT. This complex deacetylates the FOXO family of transcription factors, keeping them nuclear and promoting the expression of glucagon-induced gluconeogenic genes. Therefore, at least in liver and despite their canonical role as transcriptional repressors, class IIa HDACs can also act as transcriptional co-activators by recruiting a deacetylating function on FOXO transcription factors, thus orchestrating the cellular metabolic response during fasting. From a translational medicine point of view, this discovery has important consequences, as the liver depletion of HDAC4/5/7 in a mouse model of type 2 diabetes lower fasting blood glucose levels and improve glucose tolerance,

demonstrating a key role for class IIa HDACs in controlling glucose homeostasis (Mihaylova MM *et al.*, 2011). In support of the importance of class IIa HDACs/FOXOs axis, a similar module regulating lipid storage have been discovered in *Drosophila melanogaster* by Wang and collaborators. In their work, they reported that, in the fat body – the *Drosophila* analogue of liver and adipose tissue in mammals – of fed animals, insulin-activated Akt physically interacts with and phosphorylates Salt Inducible Kinase 3 (SIK3), another LKB1-activated metabolic responsive serine/threonine kinase belonging to the AMPK family. Once activated, SIK3 phosphorylates class IIa HDACs provoking their cytoplasmic sequestration and preventing FOXO deacetylation. Through this mechanism, acetylated FOXO is kept in the cytoplasmic compartment and, therefore unable to trigger the expression of the brummer lipase, thus promoting lipid storage. This observation was confirmed also in mammals, where insulin and glucagon impinge on two different kinases – Akt and PKA, respectively – that converge their activity on SIK2 with opposite outcomes depending on the phosphorylation sites: Akt phosphorylation of SIK2 determines its activation, whereas SIK2 phosphorylation by PKA implies its inactivation. When inactive, SIK2 is not able to phosphorylate HDAC4. Hence it can enter into the nucleus where, by deacetylating FOXO, collaborates to the induction of lypolytic (ATGL) or gluconeogenic (Pck1, G6Pase) genes (Wang B *et al.*, 2011). These findings highlight how changes in hormonal balance, which occur in different cellular metabolic requirements, can take advantage of class IIa HDACs nuclear/cytoplasmic shuttling upon phosphorylation by metabolic responsive kinases to orchestrate the cellular metabolic adaptation.

Very recently it has been found that, in human glioblastoma cell lines, mTORC2 is also able to regulate class IIa HDACs subcellular localization by phosphorylation. Again, the nuclear exclusion of class IIa HDACs has an impact on FOXOs (FoxO1 and FoxO3) acetylation. The subsequent cytosolic sequestration of FOXOs prevents these transcription factors from enhancing the transcription of a specific miRNA (mir-34c), which targets c-Myc. c-Myc stabilization is responsible for the Warburg effect well evident in GBM cells, thus rendering GBM cells exquisitely sensitive to glycolysis inhibition (Masui K *et al.*, 2013).

In addition to the role of class IIa HDACs in the regulation of metabolic genes at the transcriptional level through the modulation of the activity of specific transcription factors, some evidences have linked class IIa HDACs to the direct regulation of key

metabolic proteins through post-translational modifications. One of such proteins is the Hypoxia Inducible Factor 1α (HIF1α), a transcription factor that is constantly translated but, in condition of normoxia, is hydroxylated by oxygen-dependent prolyl-hydroxylases (PHDs) and rapidly ubiquitylated and targeted for the proteasomal degradation by the Von Hippel-Lindau (VHL) E3 ligase complex. When stabilized by low oxygen concentration, HIF1α is able to translocate into the nucleus where it dimerizes with HIF1β and to engage the transcriptional program that involves the expression of glycolytic enzymes, glucose transporters and inhibitors of the Kreb cycle. All these activities switch the metabolic phenotype of the cell toward a glycolytic one in order to cope with hypoxia. In the UMRC2 renal carcinoma cell line, defective for VHL, it has been discovered that, both class IIa (HDAC4) and class IIb (HDAC6) HDACs can physically interact with HIF1α. Their knockdown results in the reduction of HIF1α protein levels and transcriptional activity. However, only the silencing of HDAC4 determines an increase in HIF1α acetylation. In summary, by deacetylating HIF1α, HDAC4 can increase HIF1α protein stability, avoiding its proteasomal degradation even in a VHL defective context (Qian DZ *et al.*, 2006). Some years later, the same group identified a set of lysine residues at the very N-terminal region of HIF1α as the target for HDAC4 deacetylation in VHL-competent prostate (C42B) and liver (Hep3Bc1) cancer cell lines. Interestingly, the deacetylating activity against HIF1α seems to be specific for HDAC4, despite its reduced enzymatic activity versus acetyl-lysines, since the silencing of class I HDACs did not influence the acetylation level of HIF1α. Importantly, in these cancer cell lines exposed to hypoxia, down-regulation of HDAC4 decreased the expression of cancer-relevant genes such as the glucose transporter Glut1 and the lactate dehydrogenase LDHA in order to promote the glycolytic switch in cancer cells or the VEGF for tumor neoangiogenesis (Geng H *et al.*, 2011).

Another example of how class IIa HDACs, and in particular HDAC4, can modulate bioenergetic/biosynthetic pathways through their direct action on key metabolic proteins is represented by the enzyme 6-phosphogluconate dehydrogenase (6PGD). 6PGD is the third enzyme in the oxidative arm of the pentose phosphate pathway, which catalyses the decarboxylating reduction of 6-phosphogluconate to ribulose-5-phosphate with the concomitant production of NADPH. Consistently with the increased biosynthetic and antioxidant needs of tumor cells, the activity of this enzyme is commonly upregulated in many human cancer cells. It has been shown

that the acetylation of 6PGD increases its activity and, accordingly, 6PGD is commonly acetylated in diverse cancer and leukemia cell lines as well as in primary leukemia cells. Protein expression and lysines acetylation levels of 6PGD are important for cancer cell proliferation and tumor growth. HDAC4 can deacetylate 6PGD, thus dampening its activity. A less active 6PGD determines an accumulation of its substrate 6PG that is able to allosterically activate the glycolytic enzyme PFK resulting in elevated glycolytic rate, lactate production and ATP levels. Nevertheless, despite the increased glycolysis and ATP levels, H1299 lung cancer cells with a decreased 6PGD activity show reduced cell proliferation and tumor growth. In tumor/leukemia cells where the lysine acetylation-dependent activation mechanism of 6PGD is hijacked, 6PGD may be activated due to alterations in the protein levels of upstream regulators of the 6PGD, such as acetyltransferases (DLAT and ACAT2) and deacetylase (HDAC4), respectively (Shan C *et al.*, 2014). Interestingly, it has been discovered that, in tumor cell lines overexpressing the transcription factor Nrf2 a clear upregulation of the PPP genes such as glucose-6-phosphate dehydrogenase (G6PD), 6PGD, transketolase (TKT) and transaldolase (TALDO1) can be observed. At the molecular level, Nrf2 overexpression results in the down-modulation of miR-1 and miR-206, two micro RNAs which are directly repressed by HDAC4 and that, in turn, as a feedback loop, can target HDAC4 itself (Singh A *et al.*, 2013).

The following table summarize some representative evidences linking class IIa HDACs to the modulation of cellular metabolism.

Model	**Evidence**	**Reference**
Human primary myotubes	Active AMPK phosphorylates HDAC5, determining its nuclear export and resulting in increased expression of GLUT4 gene.	McGee SL *et al.*, 2008
Murine adipocytes/preadipocytes and fasting mice	Forskolin increases intracellular cAMP levels, induces HDAC4 nuclear localization and downregulates the GLUT4 promoter.	Weems JC *et al.*, 2012
Human hepatocytes and mouse liver	Glucagon-dependent increase of cAMP stimulates PKA which phosphorylates and inactivates AMPK, resulting in nuclear accumulation of class IIa HDACs. Once nuclear, they deacetylate FOXO TFs contributing to	Mihaylova MM *et al.*, 2011

	gluconeogenic and glycogenolytic genes expression.	
Drosophila melanogaster fat body and mouse liver	Insulin-activated Akt phosphorylates activates SIK3/2 that, in turn, phosphorylate class IIa HDACs determining their cytoplasmic sequestration and lipid storage.	Wang B *et al.*, 2011
Human glioblastomas	mTORC2 phosphorylates and induces the cytoplasmic retention of class IIa HDACs, thus preventing FOXO TFs to promote the expression of mir34c targeting c-Myc. C-Myc stabilization contributes to the glycolytic reprogramming of U87 cancer cells.	Masui K *et al.*, 2013
Human prostate, renal and liver cancer cell lines	HDAC4 can interact with and deacetylate HIF1α, promoting its protein stability. In hypoxia conditions, the down-regulation of HDAC4 determines the HIF1α-dependent decrease of GLUT1 and LDHA gene expression.	Qian DZ *et al.*, 2006; Geng H *et al.*, 2011
Human lung cancer and leukemia cell lines	HDAC4 can deacetylate and dampen the activity of the pentose phosphate enzyme 6PGD, stimulating the glycolytic flux.	Shan C *et al.*, 2014
Murine cardiomyocytes	Inducible cardiac-specific expression of an unphosphorylatable form of HDAC5 negatively regulates the expression of key metabolic genes involved in energy generation, along with MCAD, M-CPT-I and CPT-II (fatty acid β-oxidation), ATP synthase β (oxidative phosphorylation), hexokinase II (glycolysis), glycogen phosphorylase (glycogenolysis) and PGC1α (mitochondrial biogenesis).	Czubryt MP *et al.*, 2003

Together, these experimental evidences demonstrate how complex is the involvement of class IIa HDACs in the regulation of cellular metabolism both in physiologic and pathologic conditions. Furthermore, it is evident that the pleiotropic and somethimes antithetic metabolic functions of class IIa HDACs may be explained by the different tissue-specific metabolic requirements. All these studies, although depicting a complex scenario, highlight, in the meanwhile, the importance of class IIa

HDACs as versatile regulators of cellular metabolism and as possible targets for cancer therapy.

EXPERIMENTAL BACKGROUND AND AIM

As briefly explained in the introduction section, cancer cells rely on activated metabolic pathways to promote survival and support cell proliferation that actually reprogram cancer cell metabolism (Vander Heiden MG *et al.*, 2009). Interestingly, the wiring and directional fluxes through these metabolic routes are fine tuned by signaling and transcriptional events that can be, in turn, modulated by oncogenes and tumor-suppressor genes (Levine AJ and Puzio-Kuter AM, 2010). Therefore, targeting metabolic hubs represents a promising and attractive opportunity for cancer therapy.

In recent years, the discovery of the involvement of class IIa HDACs, and in particular of HDAC4, in the regulation of pivotal metabolic enzymes and transcription factors has raised the possibility to look at this class of deacetylases as a druggable target for cancer treatment, even from a metabolic point of view (Di Giorgio E *et al.*, 2014).

Furthermore, it has been discovered a pro-tumorigenic role of HDAC4 in several human malignancies. For instance, in ovarian, colon and neuroblastoma cancer cells HDAC4 represses in an Sp1-dependent manner, p21 transcription, thus contributing to the cell cyle progression (Wilson AJ *et al.*, 2008; Mottet D *et al.*, 2009). In breast cancer the expression of class IIa HDACs positively correlates with the aggressiveness of luminal ER+ tumor subtypes (Clocchiatti A *et al.*, 2013). Recently, the oncogenic properties of HDAC4 have been rigorously confirmed in NIH-3T3 murine fibroblasts. In particular, the overexpression of a S/A phospho-resistant form of HDAC4 (HDAC4^{TM}) that displays an almost total nuclear localization, beyond causing a deep change in cellular morphology and cytoskeleton organization, confers proliferative advantage to murine fibroblasts with respect to wild type HDAC4-infected cells in-vitro and elicits pro-tumoral functions in-vivo (Di Giorgio E *et al.*, 2013).

Provided the increasing relevance that cancer metabolism is gaining as a therapeutic option and the involvement of class IIa HDACs in the control of tumor metabolic homeostasis and tumor growth (Mihaylova MM *et al.*, 2011; Wang B *et al.*, 2011, Masui K *et al.*, 2013), the aim of this thesis is to characterize the metabolic phenotype of NIH3T3-HDAC4^{TM} tumorigenic cell line. During the PhD thesis, I studied the metabolic alterations induced by the overexpression of this “super-repressor” HDAC4 mutant, with particular attention to the “Warburg effect” typical features, namely increased glycolysis and downregulated mitochondrial metabolism.

The expected results could help to better understand the contribution of HDAC4 to metabolic reprogramming in cancer cells and to address future research for therapeutic intervention.

MATERIALS AND METHODS

Cell culture and reagents

NIH-3T3 cells were routinely grown in high glucose (4,5 g/L) Dulbecco modified Eagle medium (DMEM) (Lonza). For the lactate quantification experiments, the DMEM without phenol red was purchased from Lonza. For the cell proliferation experiments with low glucose concentration (1 g/L), the DMEM low glucose from Sigma-Aldrich was used. All culture media were provided with 1 mM sodium pyruvate and supplemented with 10% fetal bovine serum (FBS), 2 mM L-glutamine, 100 U/mL penicillin and 100 µg/mL streptomycin (Lonza).

The following reagents were used: 2-deoxy-D-glucose (2-DG) and sodium oxamate at working concentrations specified in the text, 2 µM oligomycin A, 10 µM resazurin, 0,5 mg/mL [3-(4,5-dimethyl-2-thiazolyl)-2,5-diphenyl-2H-tetrazolium bromide] (MTT), 1X protease inhibitor cocktail (PIC), 1 mM phenylmethanesulfonyl fluoride (PMSF), 1 µM rotenone, 3,3 µM carbonyl cyanide p-trifuoromethoxy-phenylhydrazone (FCCP), 2,5 µM antimycin A, 75 µM NADH, 4 mM sodium azide, 80 µM decylubiquinone (all from Sigma-Aldrich) and 200 nM tetramethylrhodamine methyl ester perchlorate (TMRM) (from Molecular Probes).

Plasmid construction, transfection and retroviral infection

The retroviral pWZL-Hygro-flag plasmid was obtained by PCR and subsequent EcoRI-SalI/XhoI subcloning of the flag sequence with the entire MCS from pFlag5c plasmid into retroviral pWZL-Hygro construct. The cDNA encoding for human wild type or triple mutan HDAC4 were cloned into pWZL-Hygro-flag by EcoRI restriction. The correct orientation and sequence of the insert was verified. Cells expressing the different transgenes were generated by retroviral infections as previously described (Fontanini A *et al.*, 2009). Briefly, retroviral vectors carrying these transgenes or empty vectors expressing only the Hygro resistance gene were used to singularly transfect the ecotropic packaging cell line LinX-E. Transfection was performed by calcium phosphate method. At 60 hours post-transfection, viral supernatants were collected, filtered, supplemented with 8 µg/mL polybrene, and combined with fresh medium in order to infect NIH-3T3 murine fibroblasts.

Soft-agar assay

Equal volumes of 1,2% agar and DMEM were mixed to generate 0,6% base agar. A total of 1×10^5 or $3,3 \times 10^4$ NIH-3T3 were seeded in 0,3% top agar, followed by incubation at 37°C in humidified conditions. The cells were grown for 21 days, and the culture medium, containing 2-DG (at concentrations indicated in the text) or oligomycin (2 μM) was changed twice per week. Colonies were visualized by MTT staining.

pH measurement of supernatant media

A total of $1,5 \times 10^4$ cells were seeded in Petri dishes and counted every 2 days. In parallel, the supernatant medium was collected and its pH immediately measured by mean of a pH meter.

Extracellular lactate quantification

A total of 1×10^5 cells were seeded in 12-well plate. After 24 hours, the culture media were substituted with complete media without phenol red and, after other 24 hours, the lactate amount in supernatant media was quantified using lactate colorimetric/fluorometric assay kit (BioVision) following manufacturer's instructions. Briefly, the supernatant media were passed through a 30 KDa cut-off Vivaspin (Sartorius) to remove serum LDH and 2 μL of the 1:10 dilution of the filtrates were diluted in 100 μL of assay buffer in 96-well plate. Then, 50 μL of the reaction mix/well were added and, after 30 minutes incubation, the colorimetric intensity was measured at 570 nm using EnSpire multimode plate reader (Perkin-Elmer). The lactate concentration was calculated by comparison with a titration curve performed with the provided lactate standard and normalized on total cell number.

Resazurin assay and IC_{50} calculation

A total of 5×10^4 cells/well were seeded in 48-well plate and, after 24 hours, the cells were treated with increasing doses of sodium oxamate (0, 12,5, 25, 50, 75 and 100 mM) or 2-DG (0, 1, 2,5, 5, 10, 20, 30, 40 and 50 mM). After 48 hours treatment, the culture media were substituted with complete media containing 10 μM resazurin and the cells were incubated for 95 minutes at 37°C in humidified conditions. The resazurin fluorescence was measured using EnSpire multimode plate reader (Perkin-

Elmer). The relative fluorescence values were interpolated with a linear regression to calculate the IC_{50} of oxamate and of 2-DG using GraphPad Prism software.

Intracellular ATP quantification

A total of 1×10^4 cells/well were seeded in a Viewplate® black 96-well (Perkin-Elmer) and grown for 36 hours. Cells were then treated with 25 mM 2-DG or 2 µM oligomycin for 1 hour at 37°C in humidified conditions. The intracellular ATP content was determined using ATP-Lite kit (Perkin-Elmer) following manufacturer's instruction. Briefly, 50 µL of lysis buffer were added to each well and, after 5 minutes shaking, 50 µL of luciferase solution per well were added. The resulting bioluminescence was detected using EnSpire multimode plate reader (Perkin-Elmer).

High resolution respirometry

Mitochondrial oxygen consumption, measured in intact cells under conditions of physiological substrate supply, was performed at 37°C using a high resolution respirometer Oxygraph 2k (Oroboros instruments, Innsbruck, Austria). Routine respiration (R) was measured in 3×10^6 cells in 3 mL chambers containing culture medium, while the leak respiration (L) was obtained in the presence of oligomycin (2,5 µg/mL), which inhibits ATP synthase; consequently, the electron flow reflects the energy requirement to compensate the futile circle of proton pumping. The maximal uncoupler–stimulated respiratory activity (E), measured in the presence of a concentration of the uncoupler FCCP (carbonyl cyanide p-trifuoromethoxy-phenylhydrazone) empirically determined as optimal (3,3 µM), provides a measure of the capacity of the electron transport system (ETS). 1 µM rotenone (which inhibits complex I) and 2,5 µM antimycin A (which inhibits complex III) were used to determine the non mitochondrial oxygen consumption. This rate was subtracted from cell total oxygen consumption to assess the mitochondrial respiration. Data were digitally recorded using DatLab4 software; oxygen flux was calculated as the negative time derivative of the oxygen concentration, $-d[O_2](t)$. A standard correction was performed for instrumental background oxygen flux arising from oxygen consumption of the oxygen sensor and minimal back-diffusion into the chamber.

Mitochondrial DNA quantification

Total (genomic plus mitochondrial) DNA was extracted starting from 3×10^6 cells using DNeasy Blood and Tissue kit (Qiagen), following manufacturer's instructions. Real-time quantitative PCR (qPCR) analysis was performed starting from 50 ng of total DNA using Bio-Rad CFX96 and SYBR green technology. ATP6 and ND4 genes were chosen as representative for mitochondrial DNA. The data were analyzed by use of a comparative threshold cycle using β2-microglobulin as normalizer gene representative for genomic DNA. The primers employed for this analysis are reported in the following table.

mouse ATP6 for	TCCCATCCTCAAAACGCCTA
mouse ATP6 rev	CCAGCTCATAGTGGAATGGC
mouse ND4 for	CCCCTTCATCCTTCTCTCCC
mouse ND4 rev	AGGAGTGATGATGTGAGGCC
mouse β2m intron for	TGAGGCTTATTGCAATGCTG
mouse β2m intron rev	ATGGCGGTTACAGTCCAAAG

Mitochondrial membrane potential (ΔΨm) quantification

Collected cells were incubated in phosphate buffer containing 200 nM TMRM and 200 nM cyclosporine A (in order to inhibit dye export from the cells by the multidrug transporters) for 30 minutes at 37°C in humidified conditions. ΔΨm was investigated in basal conditions and in the presence of some specific inhibitors: i.e. 2 μM oligomycin or 1 μM rotenone to inhibit ATP synthase and complex I, respectively. TMRM fluorescence was analyzed on a FACScan flow cytometer (Becton Dickinson) equipped with a single 488 nm argon laser and data were acquired on a logarithmic scale using Cell Quest and analyzed with WinMDI 2.8 softwares.

Complex I activity measurement

Mitochondria-enriched fractions were obtained from the cell lines as follows: 8×10^6 cells were resuspended in mitochondrial isolation buffer (250 mM sucrose, 1 mg/mL BSA, 2 mM EDTA, 1X PIC, pH 7.4) and sonicated at ice-cold temperature (five 5 seconds pulses separated by 30 seconds intervals). The resultant homogenates were subjected to differential centrifugations: 800g and 16000g for 20 minutes. All the centrifugations were performed at 4°C. The final pellets (i.e. crude mitochondria fractions) were resuspended in 100 μL of hypotonic buffer containing 25 mM K_2PO_4,

and 5 mM $MgCl_2$, pH 7.2, freezed-and-thawed two times to disrupt mitochondrial membranes and immediately used for enzymatic analysis.

Complex I activity measurements were performed as previously reported (Barrientos A, 2002). Briefly, 10 µg of mitochondria were suspended in 200 µL of water containing 150 µM NADH, 2,5 µM antimycin A and 4 mM sodium azide with or without 1 µM rotenone. After 2 minutes, the reaction was started by adding 50 µL of 50 mM Tris-HCl, pH 8.0 containing 80 µM decylubiquinone and the decrease in absorbance at 340 nm, due to the oxidation of NADH, was monitored for 5 minutes using EnSpire multimode plate reader (Perkin-Elmer). The complex I activity was corrected for the rotenone-sensitive activity.

Immunoblot analysis

Cell lysates were obtained by scraping the cells in 2X Laemmli sample buffer completed with 2% (v/v) β-mercaptoethanol, PIC and 1mM PMSF. Cell lysates were subjected to SDS-PAGE and subsequent western blot and incubated o/n with primary antibodies. HRP-conjugated secondary antibodies were purchased from Sigma-Aldrich and the blots were developed using Super Signal West Dura substrate (Pierce). The following primary antibodies were used: mouse monoclonal anti-NDUFA9 subunit of complex I (Abcam), mouse monoclonal anti-Fp subunit of complex II (Invitrogen), mouse monoclonal anti-UQCRC2 subunit of complex III (Abcam), mouse monoclonal anti-COX IV subunit of complex IV (Abcam), rabbit polyclonal anti-β subunit of ATP synthase (Mitosciences) and rabbit polyclonal anti-PGC1α (Abcam).

RESULTS and DISCUSSION

In order to evaluate the metabolic phenotype related to the expression of the unphosphorylatable mutant of HDAC4 S246/467/632A (hereafter referred to as triple mutant HDAC4^{TM}), we took advantage of murine NIH-3T3 cell lines engineered to express four different genes. NIH-3T3 fibroblasts were retrovirally infected with pWZL-hygro plasmids encoding for: 1) the GFP, selected as control gene; 2) the GTPase defective oncogenic mutant of H-RAS (H-RAS^{G12V}) as the tumorigenic control showing the classic Warburg phenotype; 3) the GFP-tagged triple mutant of HDAC4 and 4) the GFP-tagged wild type version of HDAC4 (HDAC4^{WT}) as the direct experimental counterpart. Fluorescence imaging demonstrated that, in NIH-3T3 cells, HDAC^{WT} is excluded from nuclei because subjected to nuclear cytoplasmic shuttling, while the TM mutant has a clear nuclear subcellular localization in a high percentage of cells.

NIH3T3-GFP **NIH3T3-HDAC4^{WT}** **NIH3T3-HDAC4^{TM}**

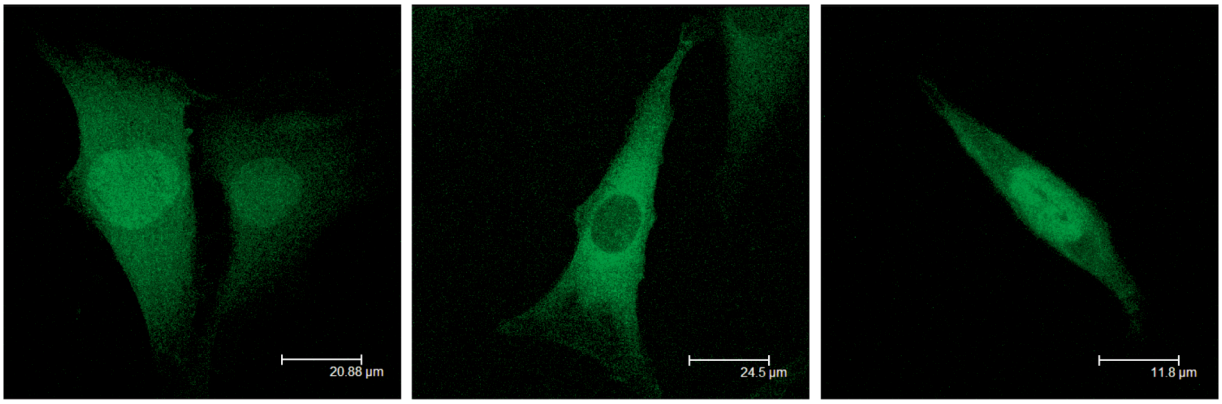

HDAC4^{TM}-driven transformation doesn't affect lactate production in NIH-3T3 cells

From the naive observation of the colour of the culture medium during the daily cell culture maintenance, or of the agar in the soft-agar assays (**figure 5A**), the clear difference in the medium acidification rate between NIH3T3-HRAS^{G12V} and NIH3T3-HDAC4^{TM} led us to hypothesize that, despite both these cell lines displayed a proliferation advantage with respect to control cells, they may differ in terms of basal metabolism. In fact, as evidenced in the soft-agar assays (**figure 5A**), the qualitative colour shift of the upper agar layer, which can be taken as a marker of

medium acidification, greatly differred between NIH-3T3 cells expressing HDAC4^{TM} and HRAS^{G12V}, although the overexpression of these mutant proteins conferred to NIH-3T3 cells a quite similar transforming potential (**figure 5B**). HDAC4^{TM}-expressing cells exhibited a tint of the phenol red indistinguishable with the non-transformed cell lines expressing GFP or the wild type version of HDAC4.

To support these qualitative data, pH measurements of conditioned media were performed. The cell growth rates were monitored every 2 days during 8 days period of culture by cell counting and, in parallel, the pH of the corresponding medium was measured using a pH meter (**figure 5C**). As previously published (Di Giorgio E *et al.*, 2013), HDAC4^{TM}-expressing cells displayed a proliferative advantage with respect to HDAC4^{WT}- or GFP-expressing cells. nevertheless they did not lower the pH of the medium that remained around 7.8. In contrast, the pH of the medium conditioned by oncogenic HRAS^{G12V}-expressing cells fell down to 6.7, as the cells grew. Notably, at the same cell density reached by HRAS^{G12V} and HDAC4^{TM} at day 6 and 8 respectively, a difference in medium pH was already observed. This data leads us to refuse the possibility that differences in the acidification of the environment could simply mirror the different number of cells growing in the Petri dish.

As already explained in the introduction section of this thesis, the augmented secretion of lactate in the extracellular environment, as consequence of increased glycolytic flux is a hallmark of Warburg-like phenotype. Therefore, we sought to analyze the lactate concentration in the extracellular environment after 2 days of cell culture (**figure 5D**). As expected, the lactate concentration in the medium of HRAS^{G12V}-expressing cells, once normalized to cell number, was almost the double when compared to GFP- and HDAC4^{WT}-expressing cells. In contrast, as expected from previous results and despite the increased proliferation rate, HDAC4^{TM}-expressing fibroblasts did not secrete more lactate in the extracellular medium. Hence, they resulted indistinguishable from un-transformed cells.

Lactate is produced by the lactate dehydrogenase (LDH) complex, which is able to convert pyruvate into lactate. This complex is composed by two subunits (LDHA and LDHB) that can combine with different stoichiometry to give rise to complexes with different enzymatic activities. LDHA, as transcriptional target of c-Myc and HIF1α, is a central player in the cellular response to hypoxia and participates in the externalization of the Warburg effect. Indeed, the inhibition of LDHA by targeted siRNA or by chemical compounds such as FX11 can halt tumor growth *in-vivo* (Lee A

et al., 2010). Moreover, as the tumoral cell progresses toward a fully transformed phenotype, it become also more sensitive to treatment with oxamate, another LDHA inhibiting small molecule, underscoring the pivotal importance of LDHA in cancer progression (Ramanathan A *et al.*, 2005). Provided these experimental evidences, we examined the dose-dependent sensibility to oxamate of our four cell lines after 48 hours treatment. The data reported in **figure 5E** demonstrate that NIH-3T3 cells overexpressing the oncogenic HRAS were generally more sensitive, in terms of growth inhibition, to oxamate treatment compared to control cells. Strikingly, the 95% confidence interval of oxamate IC_{50} for $HRAS^{G12V}$-expressing cells was significantly lower compared to the other cell lines ($38,37<IC_{50}<44,25$, $56,39<IC_{50}<67,39$, $50,42<IC_{50}<60,19$ and $50,60<IC_{50}<56,99$ for $HRAS^{G12V}$- GFP- $HDAC4^{WT}$- and $HDAC4^{TM}$-expressing cells, respectively). Furthermore, the IC_{50} of $HDAC4^{TM}$-expressing cells was not statistically different from $HDAC4^{WT}$- and GFP-expressing cells (**figure 5F**).

Together, these results demonstrate that the $HDAC4^{TM}$-induced transformation of NIH-3T3 murine fibroblasts is not coupled to increased lactate secretion, suggesting that these transformed cells are characterized by a metabolic profile that may divert in some aspects from the canonic features of the Warburg effect. In sharp contrast, as exhaustively reported in literature, oncogenic HRAS-driven transformation in fibroblasts results in the augmented lactate secretion in the extracellular space, probably as the consequence of an increased glycolytic rate, thus confirming the Warburg-like nature of the metabolic phenotype of this cell line.

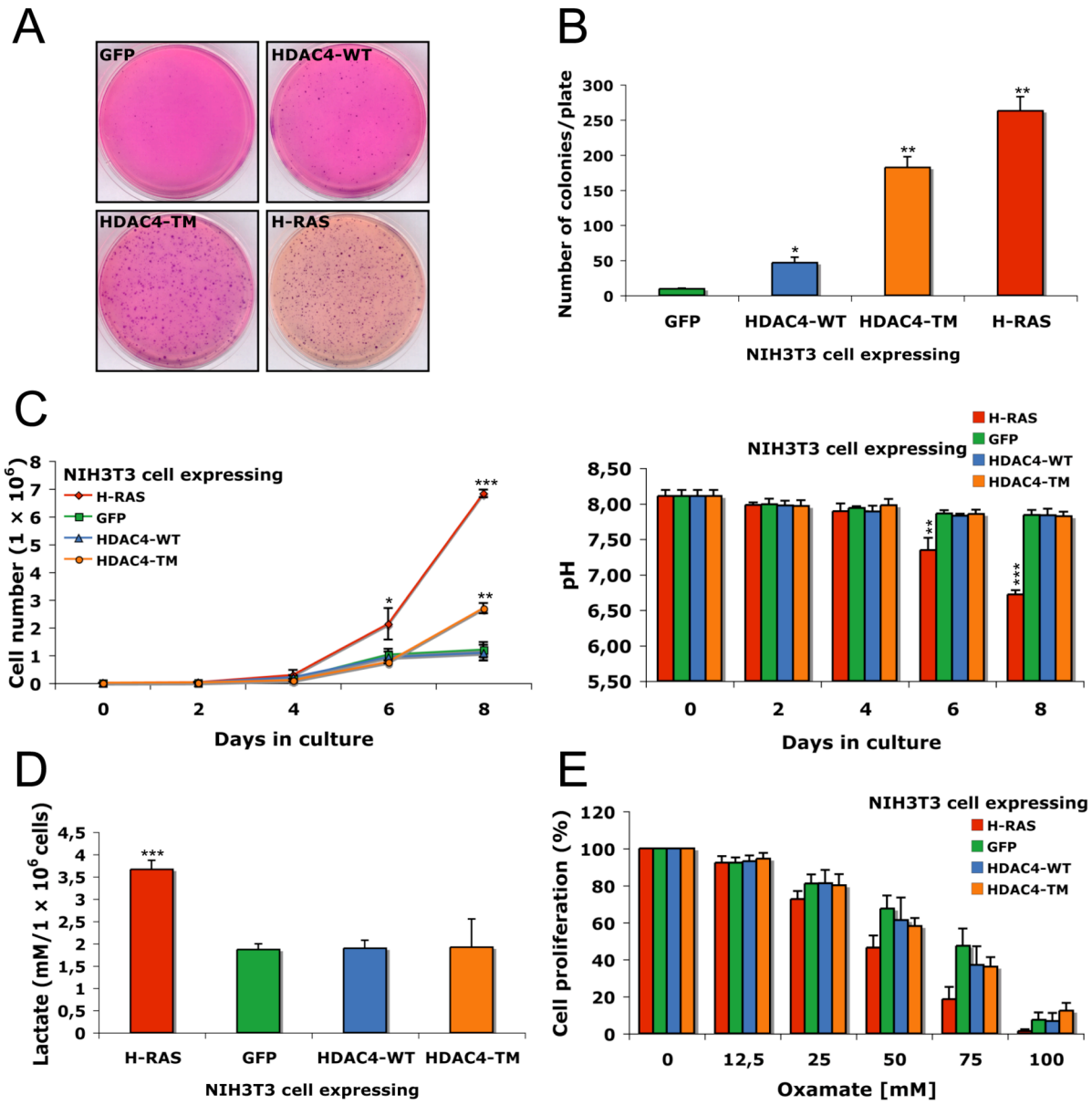

F

Oxamate [mM]		
NIH3T3 cell expressing	IC_{50}	S.D.
GFP	61,88	± 8,38
HDAC4-WT	55,49	± 11,03
HDAC4-TM	53,78	± 5,79
H-RAS	41,51	± 4,77 ***

Figure 5: HDAC4^{TM}-driven transformation doesn't affect lactate production in NIH-3T3 cells. A) Representative soft-agar assay in which 1 × 10^5 cells/plate were seeded and the transforming potential evaluated after 21 days. **B)** colonies/plate quantification of A; n = 3. **C)** Cell proliferation rate during 8 days of cell culture and concomitant measurement of medium pH; n = 3. **D)** Lactate concentration in cell medium after 48h of cell culture; n = 4. **E)** Resazurin assay of infected cells treated with different oxamate concentrations for 48h; n = 7. **F)** Oxamate IC_{50} for each cell line calculated from E. ★ = p < 0,05; ★★ = p < 0,01; ★★★ = p < 0,001 t-test statistics.

Glycolysis inhibition differentially impacts on HDAC4^{TM} and HRAS^{G12V} bioenergetics and tumorigenic potential

Since the increased glucose flux through the glycolytic pathway and the consequent metabolic reprogramming are generally recognized as common features of cancer cells, we tested the sensibility of our cell lines to glucose shortage or glycolysis inhibition. To this purpose, in a first set of experiments, the investigated cell lines were grown in media containing two different glucose concentrations: 25 mM (high glucose) or 5,56 mM (low glucose). It is important to note that in the media were present L-glutamine (5mM) and sodium pyruvate (1mM), both metabolites able to fuel mitochondrial oxidative phosphorylation for energy production. As reported in **figure 6A**, while control cells did not suffer the glucose shortage in terms of cell proliferation, even after 72h of culture, HRAS^{G12V}-expressing cells demonstrated a dramatic drop in cell number between high and low glucose conditions. This difference was already evident after 48h of glucose reduction and suggests that HRAS^{G12V}-expressing cells are more dependent on glucose for proliferation. This hypothesis is in agreement with the notion that glucose is a major source of metabolic intermediates, which can be used by cancer cells to increase, through biosynthetic pathways, their pool of building blocks for sustained proliferation. Similarly, HDAC4^{TM}-expressing cells were more sensitive to glucose shortage with respect to GFP- or HDAC4^{WT}-expressing control cells, even though to a less extent compared to HRAS^{G12V}-expressing cells. In fact, significative difference in cell numbers between high and low glucose condition was appreciable only after 72h of glucose reduction. Interestingly, in all cell lines, no substantial cell death was observed by trypan blue-positive cell counting, even after 72h of low glucose culture condition (data not shown), suggesting that glucose limitation can arrest cell proliferation without affecting cell viability. The different glucose shortage sensibility displayed by the four cell lines might reflect their diverse proliferative rates, HRAS^{G12V}-expressing cells being the most aggressive and glucose-dependent and HDAC4^{TM}-expressing cells showing an intermediate behaviour between non-transformed control cells and oncogenic HRAS control cells.
The results obtained in the glucose shortage experiments prompted us to explore the biological relevance of the main glucose-consuming metabolic pathway – the glycolysis – in conferring the proliferative advantage to fibroblasts overexpressing the phospho-resistant mutant of HDAC4. To this end, we challenged our cell lines with several concentrations of 2-deoxy-glucose (2-DG) for 48h and scored the cell

proliferation by mean of a resazurin assay. The synthetic glucose analogue 2-DG competitively inhibits glucose uptake since they are both internalized by glucose transporters. Moreover, once inside the cell, 2-DG is phosphorylated by hexokinase (HK), but the resulting 2-DG-6-P cannot be further metabolized and accumulates in the cytoplasm where non-competitively inhibits HK and competitively inhibits phospho-glucose isomerase (PGI). For these reasons 2-DG is widely used as glycolysis inhibitor in cancer therapy (Zhang D *et al.*, 2014). As reported in **figure 6B**, 2-DG treatments inhibited cell growth in all cell lines in a dose-dependent manner. However, $HRAS^{G12V}$-expressing cells displayed the highest sensibility to glycolysis inhibition when compared to untreated cells, confirming the importance of glucose metabolism in HRAS oncogenic transformation. On the other side, the non-tumorigenic GFP-expressing NIH-3T3 cells showed the lowest sensibility to 2-DG. In fact, the calculated 2-DG IC_{50} for GFP-expressing cells is more than twice that of $HRAS^{G12V}$-expressing cells (11,71 ± 0,93 mM and 5,41 ± 0,20 mM, respectively) (**figure 6C**). Here, again, $HDAC4^{TM}$-expressing cells exhibited a 2-DG sensibility in between those of non-transformed and $HRAS^{G12V}$-transformed cells. Curiously, the 95% confidence intervals of the IC_{50} of all cell lines did not overlap (data not shown), suggesting that the overexpression of HDAC4 and of its super-repressor mutant can alter the cellular dependence on glycolysis and, therefore, the cellular susceptibility to its inhibition. To reinforce these data, cells were treated for 48h with two different concentrations of 2-DG: the first equimolar to the glucose present in the culture medium (25 mM) and the second based on the previously calculated IC_{50} for $HRAS^{G12V}$-expressing cells (5 mM). Cells were then counted and we noticed that both concentrations markedly affected the proliferative advantage of oncogenic HRAS- and $HDAC4^{TM}$-expressing cells (**figure 6D**). This data, if expressed as percent with respect to not treated cells, are quite in accordance with the data obtained in the resazurin assay. Notably, neither one of the two 2-DG concentrations caused appreciable cell death after 48h treatment in any of the four cell lines, as the trypan-blue positive cells rarely exceeded the 10% (data not shown). These sets of experiments seem to suggest that the increased cell proliferation rate observed in $HRAS^{G12V}$- and $HDAC4^{TM}$-expressing fibroblasts is linked to an augmented glucose flux through glycolysis, since its inhibition results in the restoration of proliferative levels similar to those of non-tumorigenic control cell lines.

Since 2-DG is known to induce energy depletion by blocking the glycolysis pathway, we tested the impact of 2-DG treatment on intracellular ATP content. As depicted in **figure 6E**, short-term treatment (1h) of the four cell lines with 2-DG (25 mM) caused a pronounced decrease in intracellular ATP level in $HRAS^{G12V}$-expressing cells. In all the other cells lines, including the $HDAC4^{TM}$-expressing cells, 2-DG provoked a negligible reduction on the ATP levels. This result suggests that interfering with the glycolytic flux has an immediate impact on HRAS cells, which heavily rely on glycolysis for their unrestrained proliferation and hence also for energy production. It is important to keep in mind thay ATP loss caused by 2-DG-mediated glycolysis inhibition could be rescued by compensatory mechanisms, involving an up-regulation of metabolic flux through oxidative phosphorylation. In fact, when the analysis was performed after 24 hours, in $HRAS^{G12V}$-expressing cells ATP levels were similar to after 1 hour of treatment but now also in the other cells expressing GFP, $HDAC4^{WT}$ or $HDAC4^{TM}$ ATP levels were partially compromised and undistinguishable form HRAS (data not shown).

Provided the differential effects that 2-DG treatment had, as acute response, on bioenergetics between $HDAC4^{TM}$- and oncogenic HRAS-expressing cells, we asked whether glycolysis inhibition could have a similar differential impact on the long-term tumorigenic process. Therefore, in order to evaluate the tumorigenic potential of these cell lines under metabolic stress condition, we performed a series of soft-agar assays in which cells were periodically challenged with 2-DG. As reported in **figure 6F**, glycolysis inhibition by 2,5 mM 2-DG almost completely abrogated the transforming potential of both hyperactive HRAS- and $HDAC4^{TM}$-expressing cells *in-vitro*. However, using a 2-DG concentration of 1 mM in the upper medium layer, the number of colonies/plate was dramatically different between the two cell lines. In this condition, $HDAC4^{TM}$-expressing cells formed only about 30% less colonies than untreated control. In sharp contrast, HRAS-expressing cells did not develop colonies in soft-agar, similarly to the 2,5 mM 2-DG condition.

Together, these data suggest a model in which the relative dependence of the cell lines from glycolysis dictates the cellular susceptibility to glucose shortage and glycolysis inhibition. Indeed, $HRAS^{G12V}$-expressing cells, that in literature are known to be extremely glycolytic, displayed the highest sensibility to glucose shortage among the four cell lines and the lowest 2-DG IC_{50}. Moreover, in these cells, glycolysis inhibition perturbed ATP production and halted colonies formation in soft-

agar assay. On the other side, HDAC4^{TM}-expressing cells displayed an intermediate behaviour, suffering from glucose shortage only at late time points but showing a 2-DG IC_{50} lower than control cells. However, short-term glycolysis inhibition in HDAC4^{TM}-expressing cells did not alter the intracellular content of ATP in a different manner with respect to control cells. Finally their tumorigenic potential is less influenced by 2-DG compared to HRAS^{G12V} transformed cells.

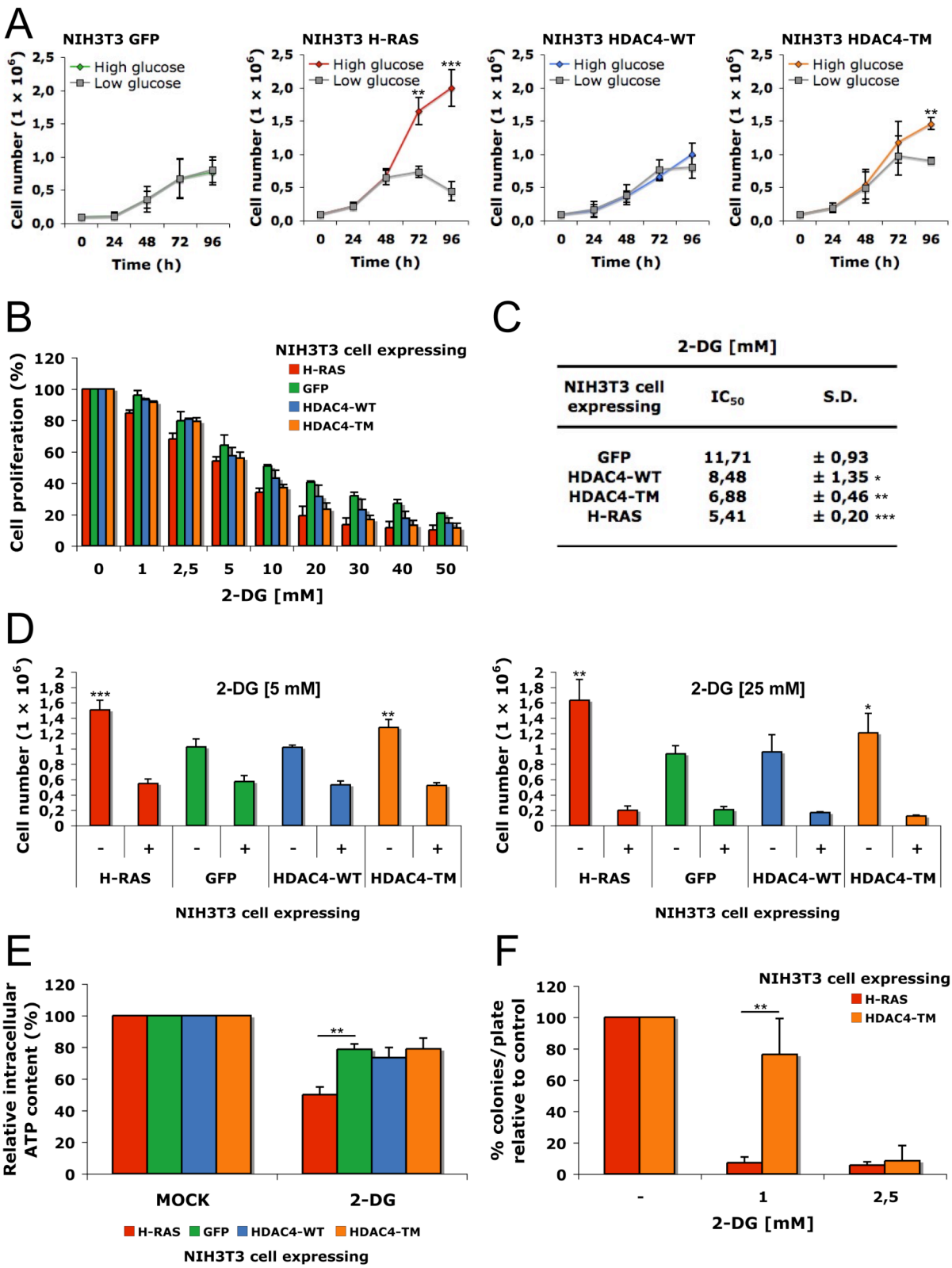

Figure 6: Glycolysis inhibition differentially impacts HDAC4^{TM} and HRAS^{G12V} bioenergetics and tumorigenic potential. A) Differential sensibility to glucose shortage of the four cell lines. 10^5 cells/plate were seeded and after 24h the cells were maintained in DMEM containing 25 mM glucose or shifted to DMEM 5,56 mM glucose for 72h and counted every 24h; n = 3. **B)** Resazurin assay of the cell lines treated with different 2-DG concentrations for 48h; n = 3. **C)** 2-DG IC_{50} for each cell line calculated from B. **D)** Cell count after 48h treatment with 2-DG at 5 mM (left) and 25 mM (right); n = 3. **E)** Intracellular ATP content of the four cell lines treated for 1h with 2-DG 25mM; n = 3. **F)** Quantification of soft-

agar experiments in which 3,3 × 10^4 cells/plate were seeded and the upper medium layer containing 2-DG (1 and 2,5 mM) changed every 3 days. The transforming potential was evaluated after 21 days; n = 3. ★ = p < 0,05; ★★ = p < 0,01; ★★★ = p < 0,001 t-test statistics.

HDAC4^{TM} overexpression does not alter mitochondrial functionality in NIH-3T3 fibroblasts

As mentioned in the introduction section, if the increased glycolysis is generally recognized as a common metabolic alteration in cancer cells, this is not always true for the concomitant down-regulation of mitochondrial oxidative phosphorylation (Hu J *et al.*, 2013; Ward PS and Thompson CB, 2012; Moreno-Sánchez R *et al.*, 2007). Therefore, in order to evaluate the overall functionality of the mitochondrial compartment in our cell lines, we determined the mitochondrial oxygen consumption. To perform these polarographic measurements we took advantage of a high resolution respirometry approach (**figure 7A**) thanks to which 3 × 10^6 intact cells for each cell line were tested for their basal (routine) respiration, the "proton-leak" respiration after the inhibition of the ATP synthase with oligomycin – in other words, the fraction of the mitochondrial oxygen consumption not coupled to ATP synthesis – and the maximal stimulated respiration after mitochondrial membrane potential collapse by the protonophore FCCP. This strategy allowed us to assess also the non-mitochondrial oxygen consumption – the residual oxygen consumption when the electron transport chain was inhibited by rotenone, antimycin A and oligomycin – but, in this case, no significative differences between the cell lines were observed (data not shown).

As shown in **figure 7B**, HRAS^{G12V}-expressing cells displayed more than 30% lower oxygen flow per cell compared to GFP-expressing control cells. This data is in good accordance with previous experimental evidences (Hu Y *et al.*, 2012) and strongly suggests that the mitochondrial compartment in this cell line may be down-modulated in basal conditions. In contrast, while HDAC4^{WT}-expressing cells did not differ from GFP control, HDAC4^{TM}-expressing cells showed even a slightly higher basal respiration rate compared to control cells, allowing to hypothesize an unperturbed or even upregulated mitochondrial compartment in the transforming HDAC4^{TM} cell line and underlining its pronounced divergence with respect to oncogenic HRAS cell line. Instead, no difference was noticed between the cell lines when we evaluated the oxygen consumption due to futile cycles not coupled to ATP synthesis (oligomycin-

insensitive leak respiration). However, when mitochondria were maximally stimulated by the protonophore FCCP titration, the maximal activity of the electron transport system displayed consistent variability between the cell lines. In particular, $HRAS^{G12V}$ cell line was characterized by the lowest maximal mitochondrial spare capacity, thus suggesting that this cell line may not be able to upregulate mitochondria in case of higher metabolic requirements. In contrast, $HDAC4^{TM}$ cell line consumed significantly more oxygen than GFP control cells in their maximal mitochondrial stimulation state. Once again, this data highlights the marked difference existing between $HRAS^{G12V}$ and $HDAC4^{TM}$ cell lines also in the mitochondrial performance. Therefore, this high resolution respirometry analysis markedly support the notion that, while hyperactive HRAS-expressing cells displayed less functional or bad-performing mitochondria, HDAC4 overexpression (both the wild type and the super-repressive forms) had a different effect on mitochondrial activity, since the oxygen consumption in the various metabolic states was comparable or even slightly higher than control GFP-expressing cells. However, when the values were normalized for the maximal respiratory capacity, the fraction of the respiration used in routine conditions to produce ATP (i.e. (R-L)/ME) did not show any difference between the cell lines. It should be emphasized that the higher ETC capacity displayed by $HDAC4^{TM}$-expressing cells respect to the control cell lines may account for a great mitochondrial plasticity in this cell line, but not in $HRAS^{G12V}$-expressing cells. In fact, by increasing the fraction of the respiration used to generate ATP, $HDAC4^{TM}$-expressing cells may better adapt to stress conditions that involve an ATP depletion. The lower susceptibility exhibited by $HDAC4^{TM}$-expressing cells to 2-DG, compared to $HRAS^{G12V}$ transformed cells (figure 6E), may be explained by such a mechanism.

Certainly, a difference in oxygen consumption between the cell lines could be explained by a variation in the number of mitochondria per cell. For this reason, we quantified the mitochondrial DNA by RT-PCR as a parameter to estimate the mitochondrial mass in each cell line (**figure 7C**). The DNA sequences coding for the NADH dehydrogenase subunit ND4 and for the ATP6 subunit of the ATP synthase were chosen as representative of mitochondrial DNA, whereas β2-microglobulin gene was used for genomic DNA normalization. This analysis revealed no obvious change in mitochondrial DNA amount among the cell lines, suggesting that the mitochondrial mass was similar between all the cell lines. This result excludes the possibility that the differences in oxygen consumption observed among the cell lines were due to

variations of mitochondrial content. To confirm these data, the protein levels of peroxisome proliferator activated receptor γ coactivator 1 α (PGC1α), a well known inducer of mitochondrial biogenesis (Vazquez F *et al.*, 2013), were assessed by western blot analysis. Also in this case, we didn't find any change in PGC1α protein expression throughout the cell lines (data not shown), reinforcing the hypothesis that a variation in the mitochondrial load was not the cause of the observed differences in oxygen consumption between the cell lines .

In order to further support the functionality of the mitochondrial compartment of HDAC4^{TM}-expressing cells, we sought to measure their mitochondrial membrane potential (MMP). To this aim, we first generated new NIH-3T3 cell lines stably expressing the flag-tagged HDAC4 proteins (both wild type and triple S/A mutant) and the counterpart empty hygromycin control, to avoid that the GFP fusion may interfere with the cytofluorimetric analysis. The effective expression of ectopic proteins was verified by western blot analysis. Next, the proliferative advantage and the tumorigenic potential of the flag-HDAC4^{TM}-expressing cells were confirmed by cell counting and soft-agar assays (data not shown). To measure the MMP, we employed a TMRM-based cytofluorimetric analysis in which the cells were stained with 200 nM TMRM in the presence or absence of 2 μM oligomycin and 1 μM rotenone (**figure 7D**). Oligomycin, by inhibiting the ATP synthase, is able to block the proton influx from the mitochondrial inter-membrane space into the matrix. Since the other proton-extruding electron transport system complexes, namely complex I, III and IV, are not perturbed and still functional working, oligomycin treatment results in the net increase of the mitochondrial membrane potential. In contrast, rotenone is a potent inhibitor of OXPHOS complex I and it can block, at least in part, the electron flux through the electron transport chain and the proton efflux from the mitochondrial matrix.

As shown in figure 7D, in basal conditions the mitochondrial membrane potential did not differ among the tested cell lines. However, when the cells were co-treated with TMRM and oligomycin, a substantial difference in fluorescence response between HRAS^{G12V} and control cells was evident, thus suggesting that a less active electron transport chain was operating upstream the ATP synthase in HRAS-expressing cells. On the contrary, no statistically significant differences were observed in oligomycin-induced MMP between HDAC4^{WT} or HDAC4^{TM} and control cells, indicating an unperturbed functionality of ATP synthesis system coupled with the electron transport

system and consuming MMP in these cell lines. Concomitant co-treatment with rotenone greatly decreased the oligomycin-induced MMP, indicating that ETC were major contributors to the maintenance of the mitochondrial membrane potential in all cell lines. However, this decrease was significatively less pronounced ($p<0,05$) in $HRAS^{G12V}$ (-67,3%) and in $HDAC4^{TM}$ (-67,1%) cells compared to control cells (-84,9% and -75,2% for 3T3-Hygro and 3T3-$HDAC4^{WT}$, respectively). This prompted us to investigate the complex I in particular, through the assessment of its catalytic activity (**figure 7E**). To this aim, the mitochondria-enriched fraction was obtained for each cell line and the complex I activity tested, as described in the Material and Methods section. Interestingly, compared to control cells, in $HRAS^{G12V}$ and $HDAC4^{TM}$ expressing cells, complex I activity was determined to be about 30% lower and 28% higher, respectively. To strengthen this data, we analyzed the protein expression of complex I (NDUFA9 subunit) by western blot (**figure 7F**) and found that it was less expressed in $HRAS^{G12V}$ cells compared to control cells, while no difference was observed in $HDAC4^{TM}$-expressing cells. No differences in the protein level of the other components of the mitochondrial electron transport chain were evident between the cell lines (data not shown). These findings are in accordance with literature data, involving a complex I dysfunction as one of the causing event contributing to the onset of the Warburg effect in oncogenic Ras cancers (Yang D *et al.*, 2010; Baracca A *et al.*, 2010; Palorini R *et al.*, 2013). Moreover, together with the data regarding the MMP, these data support the hypothesis that in $HRAS^{G12V}$-expressing cells, the complex I reduced activity likely caused an electron transport system defect leading to mitochondrial OXPHOS down-regulation. By contrast, in $HDAC4^{TM}$-expressing cells exhibiting a normal (or slightly higher) complex I activity, the low decrease of the oligomycin-induced MMP caused by concomitant treatment with rotenone, mimicking an apparent low contribution of complex I to MMP, may be speculatively explained by a compensatory up-regulation of complex II that can allow the other proton-pumping ETS complexes, namely complex III and IV, to function.

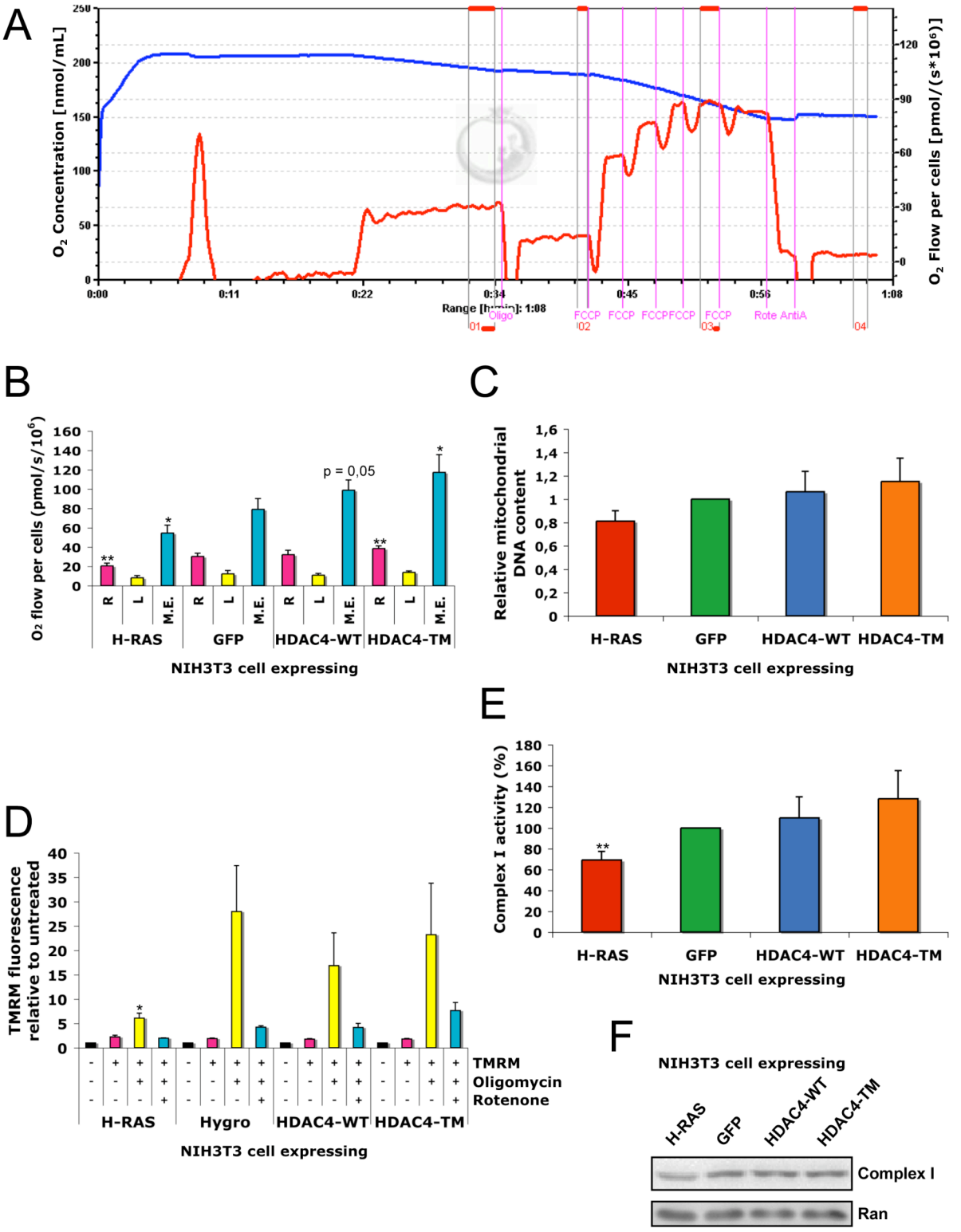

Figure 7: HDAC4^{TM} overexpression does not alter mitochondrial functionality in NIH-3T3 fibroblasts. A) Representative output of a typical high resolution respirometry analysis: 3 × 10^6 cells were transferred in complete medium into the polarographic chamber and the oxygen consumption in basal condition was recorded after the flow equilibrium was reached. 2,5 µg/mL oligomycin were then added to measure the proton-leak respiration and a titration with the protonophore FCCP was performed to evaluate the maximal uncoupler-stimulated respiratory activity that was reached at 3,3 µM FCCP. No-mitochondrial oxygen consumption was obtained by adding rotenone (1 µM) and antimycin A (2,5 µM) and this value was

subtracted from all the previous to assess the mitochondrial-specific respiration. **(B)** Oxygen flow, measured as (pmol/(s × 10^6 cells) in routine (R), oligomycin-insensitive proton-leak (L) and maximal stimulation of the electron transport system (M.E.) conditions by high resolution respirometry; n = 4. **(C)** Relative mitochondrial DNA content quantified by RT-PCR on two mitochondrial genes (ND4 and ATP6) and normalized to genomic β2m; n = 3. **(D)** Mitochondrial membrane potential in intact cells measured by cytofluorimetric analysis after mitochondrial staining with 200 nM TMRM and co-treatment with oligomycin (2 μM) and rotenone (1 μM); n = 3. **(E)** Relative electron transport system complex I activity biochemically determined as reported in the Materials and Methods section; n = 3. **(F)** Representative immunoblot of complex I protein level. All the statistical significancies have been calculated with respect to GFP-expressing or Hygro control 3T3 cells. ★ = $p < 0,05$; ★★ = $p < 0,01$; ★★★ = $p < 0,001$ t-test statistics.

Mitochondrial ATP synthesis inhibition by oligomycin does not abolish the tumorigenic potential of HDAC4^{TM}-expressing cells

Given the unperturbed functionality of mitochondrial oxidative phosphorylation in HDAC4^{TM}-expressing fibroblasts, we wondered if OXPHOS inhibition would hamper their tumorigenic potential. To test this hypothesis, we first evaluated the impact of oligomycin treatment on the intracellular ATP content. As reported in **figure 8A**, 1h treatment with 2 μM oligomycin did not affect the intracellular ATP amount in none of the cell lines. Similar results were obtained also when the treatment duration was prolonged to 2 and 24h (data not shown). This could reflect compensatory mechanisms aimed to restore the oligomycin-induced ATP depletion, which are operating in all cell lines, as already reported by other authors using different electron transport chain inhibitors in oncogenic HRAS and normal NIH-3T3 cells (Yang D *et al.*, 2010). However, these data are partially in contrast with previous published results where an oligomycin-provoked effect on ATP production was observed even after 24h treatment in KRAS and normal NIH-3T3 fibroblasts (Palorini R *et al.*, 2013). Nonetheless, we sought to investigate the impact on cellular proliferation upon long-term oligomycin treatment (**figure 8B**). Strikingly, 48h treatment of HDAC4^{TM}-expressing cells with 2 μM oligomycin affected the proliferative advantage that this cell line exhibited with respect to untreated control cells. The same treatment, although reduced the proliferative index of HRAS^{G12V}-expressing cells, did not cancel the proliferative advantage of these transformed cells. Therefore, oligomycin treatment, in this experimental setting, had a lower impact on HRAS^{G12V}- than on HDAC4^{TM}-expressing cells (i.e. 28,53% versus 43,98% decrease in cell proliferation, respectively), in line with their mitochondrial profiles.

Prompted by these results, we examined by soft-agar assays the *in-vitro* tumorigenic potential of hyperactive HRAS- and HDAC4^{TM}-expressing cells when challenged with repeated pulses of oligomycin for the entire duration of the experiment (**figure 8C**). It should be noted that 2 μM oligomycin treatment still permitted the colony growth of both HRAS^{G12V}- and HDAC4^{TM}-expressing cells, in contrast to what observed with the 2-DG treatment at 25 and 5 mM, where no colonies were present in none of these cell lines (data not shown). Oligomycin treatment hampered the ability to grow in anchorage-independent way in both cell lines but, unexpectedly, had a higher impact on the tumorigenic potential of HRAS^{G12V}- respect to HDAC4^{TM}-expressing cells. These apparently puzzling results highlight how complex could be the response of cells exposed to chronic metabolic inhibition, and may be explained by different adaptive mechanisms likely occurred with a different time-scale. In fact, although HDAC4^{TM}-expressing cells, being mitochondrially competent, showed an oligomycin impact on cell proliferation higher than HRAS^{G12V}- expressing cells within 48 hours, they could be able to respond to the constraint on oxidative phosphorylation imposed by oligomycin treatment by the activation/up-regulation of glycolytic flux. Such a response has been recently suggested in other "oxidative" cancers (Lim JH *et al.*, 2014). In other words, the glycolytic reserve capacity of HDAC4^{TM}-expressing cells could be, similarly to their mitochondrial competence, as their normal counterparts (i.e. HDAC4^{WT} and GFP-expressing cells). This hypothesis is corroborated by the empirical observation in the three cell lines of a slight change of color of the phenol-red toward the acidic pH upon oligomycin treatment, either in the culture medium or in the upper agar layer (data not shown). In addition, we may hypothesize that, in principle, the long-term blockade of ATP synthase caused a cumulative ROS production exceeding, in the 21 days time-scale, the cellular repair capability and leading to cell death. Such an effect may be more invasive in the hyperactive HRAS context where ROS over-production is reported as elevated per se (Kopnin PB *et al.*, 2007; Weinberg F *et al.*, 2010), thereby explaining the higher impact observed on the tumorigenic potential of HRAS^{G12V}- respect to HDAC4^{TM}-expressing cells. It should be emphasized that preliminary results (not shown), obtained by assessing intracellular ROS levels in basal conditions by H_2-DCF-DA fluorescence, documented a 25% higher intracellular ROS in HRAS^{G12V}-expressing cells compared to not transformed fibroblasts. In contrast, HDAC4^{TM}-expressing cells did not show a significative difference in intracellular ROS levels with respect to both HDAC4^{WT}-

expressing or Hygro-control cells. These results, although very preliminary, may support our latter hypothesis and prompt us to investigate the possible preventive effects of antioxidants such as NAC, as well as to detect markers of oxidative damage and intracellular ROS generation following oligomycin treatment.

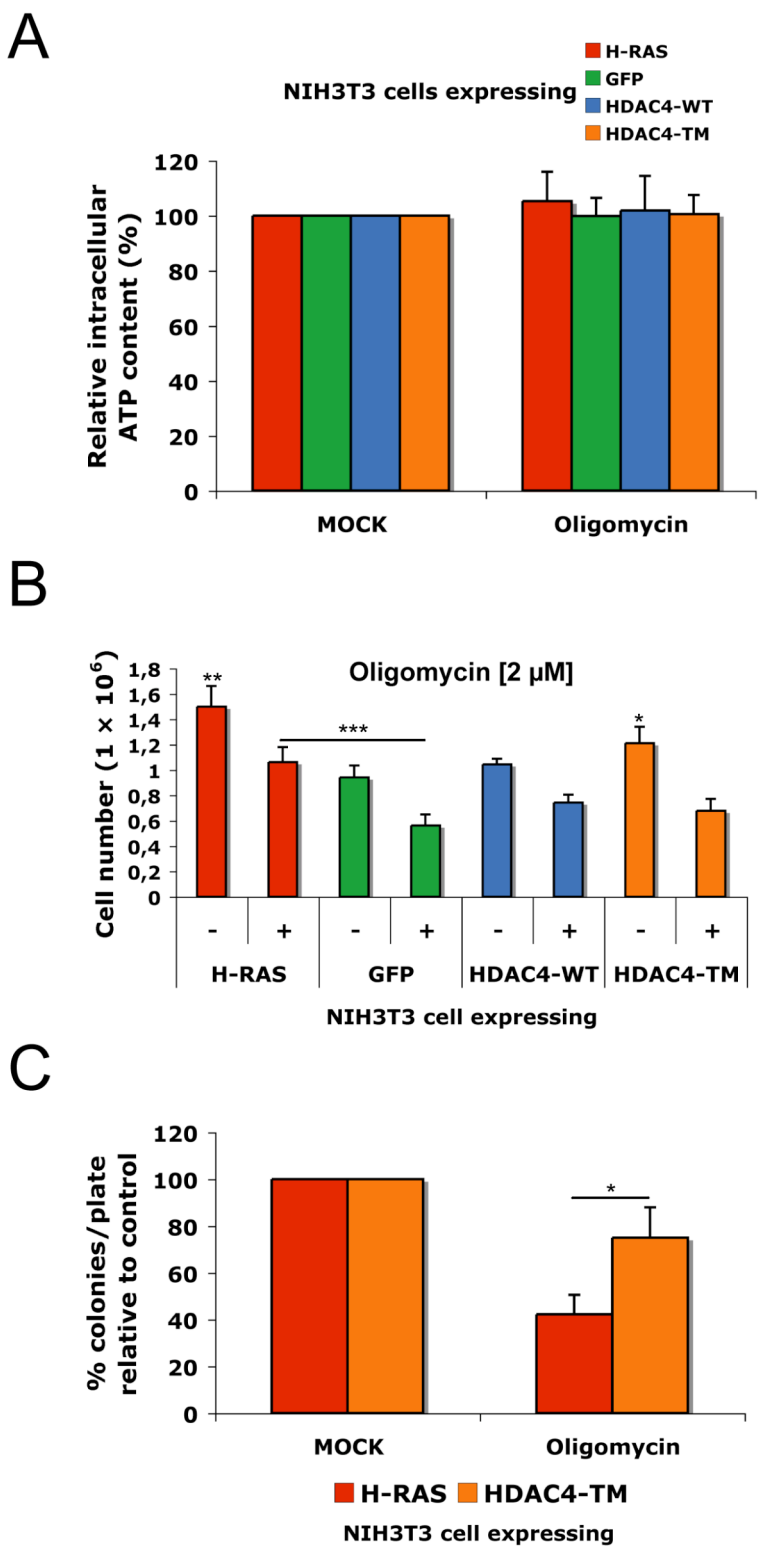

Figure 8: Mitochondrial ATP synthesis inhibition by oligomycin abolishes HDAC4^{TM} proliferative advantage, but not its tumorigenic potential. A) Intracellular ATP content of the four cell lines treated for 1h with 2 µM oligomycin; n = 3. **B)** Cell count after 48h treatment with 2 µM oligomycin; n = 4. **C)** Quantification of soft-agar experiments in which 3,3 × 10^4 cells/plate were seeded and the upper medium layer containing 2 µM oligomycin changed every 3 days. The transforming potential was evaluated after 21 days; n = 3. ★ = p < 0,05; ★★ = p < 0,01; ★★★ = p < 0,001 t-test statistics.

CONCLUDING REMARKS

Nearly 90 years have passed since the pioneering discovery of cancer cell metabolic reprogramming (Warburg O, 1927) and, in the last decade, a lot of efforts have been profused to understand the molecular mechanisms governing this metabolic shift and the interconnection with oncogenes activation or tumor suppressors' loss of function. Pioneering work demonstrated that cancer cells rely mostly on enhanced glycolysis to survive and support cell proliferation. Otto Warburg proposed a possible explanation for this metabolic dependence. He identified in a mitochondrial defect, which depletes cellular energy support, the leading cause forcing cancer cells to restore ATP levels by the less efficient fermentation process (Warburg O, 1956). Unfortunately, these early observations, while remaining true for several cancer types, have led to the belief that all tumors are characterized by mitochondrial compartment down-regulations. In fact, it was demonstrated that, in most cancer cells, mitochondria are actually reprogrammed to contribute, through cataplerotic mechanisms, to the synthesis of macromolecules necessary for tumor cell growth (DeBerardinis RJ *et al.*, 2007) and that mitochondrial oxidative phosphorylation can be still operative (Hu J *et al.*, 2013; Moreno-Sánchez R *et al.*, 2007), even if the carbon source used to fuel the TCA cycle may be shifted from glucose to glutamine (Fan J *et al.*, 2013).

In this thesis, we have addressed the question whether the transformation induced in NIH-3T3 murine fibroblasts by the overexpression of a "super-repressor", phospho-resistant mutant form of HDAC4 could present the typical metabolic features characterizing the Warburg phenotype. We have demonstrated that the proliferative advantage of HDAC4^{TM}-expressing cells was not accompanied by an increase in extracellular lactate secretion, a hallmark of the Warburg effect, instead it was evident in oncogenic HRAS-expressing cells. Therefore, despite a quite similar tumorigenic potential, HDAC4- and HRAS-driven tumorigenesis greatly differ in terms of lactate production and sensibility to lactate dehydrogenase chemical inhibition, as demonstrated by the statistically significant difference in oxamate IC_{50} between the cell lines. Nevertheless, we have found that HDAC4^{TM}-expressing fibroblasts are also more sensible, compared to normal cells, to both glucose shortage and 2-DG-mediated glycolysis inhibition, even if to a less extent compared to HRAS^{G12V}-expressing cells. These data could suggest that, in HDAC4^{TM} cells, the glucose flux

through glycolytic route is increased in order to speculatively provide a higher amount of glycolytic intermediates for the biosynthesis of cellular components and sustain cell proliferation. In fact, when glycolysis is blocked the proliferative advantage of HDAC4^{TM} cells is lost. However, in HRAS^{G12V}-expressing cells glycolysis up-regulation is even higher thus leaving open the possibility that the excess of pyruvate produced is disposed through fermentation and lactate secretion. The higher levels of glycolysis in HRAS were confirmed by the decrease in intracellular ATP content following acute 2-DG treatment and by the differential 2-DG dose-dependent tumorigenic response compared to HDAC4^{TM} cells.

As a matter of facts, the higher rate of glycolysis observed in oncogenic HRAS cells can be, at least in part, justified and, in a certain way, constrained by a defect at mitochondrial level. We have determined, indeed, that most parameters that we have used to evaluate mitochondrial functionality resulted downregulated in HRAS^{G12V}-expressing cells, as already reported in several papers (Yang D *et al.*, 2010; Rimessi A *et al.*, 2014). In particular, we have observed a down-modulation of OXPHOS complex I, both at the activity and protein expression level in HRAS^{G12V} cells, as also reported in literature for other oncogenic Ras isoforms (Baracca A *et al.*, 2010). This may explain why in HRAS^{G12V} cells we have measured a lower mitochondrial-specific oxygen consumption, both in basal condition and when the mitochondria were maximally stimulated by mitochondrial membrane collapse. In this regard, the decreased activity and/or protein expression of OXPHOS complex I could be also responsible for the lower mitochondrial membrane potential increase detected in hyperactive HRAS cells when the proton influx toward the mitochondrial matrix was blocked by oligomycin-mediated ATP synthase inhibition. Together, these data point to a general down-regulation of the mitochondrial compartment in the oncogenic HRAS context, even though it is not yet clear if this mitochondrial defect would be a causing event or simply a consequence of the aerobic glycolysis displayed by these cancer cells.

In sharp contrast, we did not detect any particular mitochondrial impairment in HDAC4^{TM}-expressing fibroblasts. In this cell line, all the mitochondrial parameters tested were within the normal range or even slightly higher, as in the case of the oxygen consumption, indicating that the increased glycolytic flux observed was not the result of a compensatory molecular mechanism to restore cellular bioenergetics. Although a well performing oxidative phosphorylation in HDAC4^{TM} cells, we did not

notice appreciable depletion of ATP content following oligomycin treatment, probably because, during the 1 hour period of ATP synthase inhibition, an up-regulation of other ATP-generating pathways (glycolysis) could account for the ATP level restoration, as previously reported (Yang D *et al.*, 2010). However, longer inhibition (48 hours) of mitochondrial oxidative phosphorylation efficiently blunted the proliferative advantage of HDAC4^{TM}-expressing cells, whereas had a much limited effect on oncogenic HRAS cell growth. Unexpectedly, this finding was not confirmed when we have scored the tumorigenic potential of these cell lines, once challenged with oligomycin pulses for the entire duration of the soft-agar assays (21 days). It is likely that differences in the ability of HRAS^{G12V} and HDAC4^{TM} cells to mount compensatory metabolic mechanisms, such as an increase in glycolysis, in order to face the block of oxidative phosphorylation can account for the different clonogenic potential displayed by these cell lines upon oligomycin treatment, as already proposed (Lim JH *et al.*, 2014).

Altogether, these data have highlightened a marked metabolic difference, the classical Warburg effect, between HRAS and HDAC4^{TM} transformed fibroblasts. In conclusion, the data support the hypothesis that HDAC4-driven tumorigenic process is characterized by increased glucose dependence and glycolysis, as the vast majority of cancers, but, in contrast to HRAS-driven tumors, does not show the typical Warburg phenotype because the augmented glycolysis is not coupled to a concomitant increase in lactate secretion and no obvious mitochondrial defects are present in transformed fibroblasts. Interestingly, it was discovered that in rat fibroblasts, the exogenous expression of KRAS^{G12V} led to the γ-catenin/Lef1-mediated transcriptional down-regulation of HDAC4 and that the re-expression of HDAC4 had a dramatic effect on the invasive, migratory and motility ability of KRAS^{G12V}-infected fibroblasts (Yim JH *et al.*, 2013). Moreover, Wang and colleagues have demonstrated that, in a microglial cellular model challenged with LPS, high level of glycolysis are responsible for the caspase-3-dependent degradation of HDAC4 and consequent modulation of pro-inflammatory cytokines production (Wang B *et al.*, 2014). These results, however, are partially in contraddiction with those obtained in the skeletal muscle context, where class IIa HDACs have been implicated in the physiological skeletal muscle fiber determination (Potthoff MJ *et al.*, 2007). In this paper, it has been shown that the combined depletion of HDAC5 and HDAC9 or muscle-specific depletion of HDAC4 and HDAC5 in mice results in an increase of

slow-twitch oxidative fibers. Moreover, the continuous repression of MEF2 target genes by class IIa HDACs in adult skeletal muscle is sufficient to block the exercise-induced switch from glycolytic to oxidative muscle fibers *in-vivo*. Infact, from a functional point of view, in slow, oxidative muscle fibers, class IIa HDACs are ubiquitylated in the nucleus and rapidly degraded through the proteasome system (Potthoff MJ *et al.*, 2007). Recently, these results have been confirmed by another research group which demonstrated that the phosphorylation status of HDAC4, through the repression of MEF2-dependent, PGC1α-mediated oxidative metabolic gene program, contributes to the establishment of muscle fiber type-specific transcriptional programs (Choen TJ *et al.*, 2015).

These results illustrate the tissue-specific nature and the pleiotropic roles that HDAC4 can play as a versatile connector between cell metabolism and the response to stimuli, both in physiological and pathological conditions. This complexity fully justifies the need of future rigorous studies on HDAC4 and metabolism, which were only preliminary addressed with this thesis. It is evident that understanding this connection will help to better explore the possibility of pharmacologically target HDAC4 for the metabolic modulation of cancer cells as a therapeutic strategy.

BIBLIOGRAPHY

1)	Inhibition of AMPK and Krebs cycle gene expression drives metabolic remodeling of Pten-deficient preneoplastic thyroid cells. **Antico Arciuch VG**, Russo MA, Kang KS, Di Cristofano A. Cancer Res. 2013 Sep 1;73(17):5459-72. doi: 10.1158/0008-5472.CAN-13-1429. Epub 2013 Jun 24.
2)	Selective repression of MEF2 activity by PKA-dependent proteolysis of HDAC4. **Backs J**, Worst BC, Lehmann LH, Patrick DM, Jebessa Z, Kreusser MM, Sun Q, Chen L, Heft C, Katus HA, Olson EN. J Cell Biol. 2011 Oct 31;195(3):403-15. doi: 10.1083/jcb.201105063.
3)	Mitochondrial Complex I decrease is responsible for bioenergetic dysfunction in K-ras transformed cells. **Baracca A**, Chiaradonna F, Sgarbi G, Solaini G, Alberghina L, Lenaz G. Biochim Biophys Acta. 2010 Feb;1797(2):314-23. doi: 10.1016/j.bbabio.2009.11.006. Epub 2009 Nov 18.
4)	In vivo and in organello assessment of OXPHOS activities. **Barrientos A**. Methods. 2002 Apr;26(4):307-16. Review.
5)	Structural and functional analysis of the human HDAC4 catalytic domain reveals a regulatory structural zinc-binding domain. **Bottomley MJ**, Lo Surdo P, Di Giovine P, Cirillo A, Scarpelli R, Ferrigno F, Jones P, Neddermann P, De Francesco R, Steinkühler C, Gallinari P, Carfí A. J Biol Chem. 2008 Sep 26;283(39):26694-704. doi: 10.1074/jbc.M803514200. Epub 2008 Jul 8.
6)	mTOR- and HIF-1α-mediated aerobic glycolysis as metabolic basis for trained immunity. **Cheng SC**, Quintin J, Cramer RA, Shepardson KM, Saeed S, Kumar V, Giamarellos-Bourboulis EJ, Martens JH, Rao NA, Aghajanirefah A, Manjeri GR, Li Y, Ifrim DC, Arts RJ, van der Veer BM, Deen PM, Logie C, O'Neill LA, Willems P, van de Veerdonk FL, van der Meer JW, Ng A, Joosten LA, Wijmenga C, Stunnenberg HG, Xavier RJ, Netea MG. Science. 2014 Sep 26;345(6204):1250684. doi: 10.1126/science.1250684. Erratum in: Science. 2014 Nov 7;346(6210):aaa1503. van der Meer, Brian M J W [corrected to van der Veer, Brian M J W].
7)	Expression of transforming K-Ras oncogene affects mitochondrial function and morphology in mouse fibroblasts. **Chiaradonna F**, Gaglio D, Vanoni M, Alberghina L. Biochim Biophys Acta. 2006 Sep-Oct;1757(9-10):1338-56. Epub 2006 Aug 3.
8)	New Insights into the Connection Between Histone Deacetylases, Cell Metabolism, and Cancer. **Chiaradonna F**, Cirulli C, Palorini R, Votta G, Alberghina L. Antioxid Redox Signal. 2014 Mar 6. [Epub ahead of print]
9)	The M2 splice isoform of pyruvate kinase is important for cancer metabolism and tumour growth. **Christofk HR**, Vander Heiden MG, Harris MH, Ramanathan A, Gerszten RE, Wei R, Fleming MD, Schreiber SL, Cantley LC. Nature. 2008 Mar 13;452(7184):230-3. doi: 10.1038/nature06734.
10)	HDAC4 Regulates Muscle Fiber Type-Specific Gene Expression Programs. **Cohen TJ**, Choi MC, Kapur M, Lira VA, Yan Z, Yao TP. Mol Cells. 2015 Feb 25. doi: 10.14348/molcells.2015.2278. [Epub ahead of print]
11)	Class IIa HDACs repressive activities on MEF2-depedent transcription are associated with poor prognosis of ER^+ breast tumors. **Clocchiatti A**, Di Giorgio E, Ingrao S, Meyer-Almes FJ, Tripodo C, Brancolini C. FASEB J. 2013 Mar;27(3):942-54. doi: 10.1096/fj.12-209346. Epub 2012 Nov 16.
12)	Regulation of peroxisome proliferator-activated receptor gamma coactivator 1 alpha (PGC-1 alpha) and mitochondrial function by MEF2 and HDAC5. **Czubryt MP**, McAnally J, Fishman GI, Olson EN. Proc Natl Acad Sci U S A. 2003 Feb 18;100(4):1711-6. Epub 2003 Feb 10.
13)	Calcium/calmodulin-dependent protein kinase activates serum response factor transcription activity by its dissociation from histone deacetylase, HDAC4. Implications in cardiac muscle gene regulation during hypertrophy. **Davis FJ**, Gupta M, Camoretti-Mercado B, Schwartz RJ, Gupta MP. J Biol Chem. 2003 May 30;278(22):20047-58. Epub 2003 Mar 26.

14)	Beyond aerobic glycolysis: transformed cells can engage in glutamine metabolism that exceeds the requirement for protein and nucleotide synthesis. **DeBerardinis RJ**, Mancuso A, Daikhin E, Nissim I, Yudkoff M, Wehrli S, Thompson CB. Proc Natl Acad Sci U S A. 2007 Dec 4;104(49):19345-50. Epub 2007 Nov 21.
15)	The biology of cancer: metabolic reprogramming fuels cell growth and proliferation. **DeBerardinis RJ**, Lum JJ, Hatzivassiliou G, Thompson CB. Cell Metab. 2008 Jan;7(1):11-20. doi: 10.1016/j.cmet.2007.10.002. Review.
16)	MEF2 is a converging hub for histone deacetylase 4 and phosphatidylinositol 3-kinase/Akt-induced transformation. **Di Giorgio E**, Clocchiatti A, Piccinin S, Sgorbissa A, Viviani G, Peruzzo P, Romeo S, Rossi S, Dei Tos AP, Maestro R, Brancolini C. Mol Cell Biol. 2013 Nov;33(22):4473-91. doi: 10.1128/MCB.01050-13. Epub 2013 Sep 16.
17)	Selective class IIa HDAC inhibitors: myth or reality. **Di Giorgio E**, Gagliostro E, Brancolini C. Cell Mol Life Sci. 2015 Jan;72(1):73-86. doi: 10.1007/s00018-014-1727-8. Epub 2014 Sep 5.
18)	Akt stimulates aerobic glycolysis in cancer cells. **Elstrom RL**, Bauer DE, Buzzai M, Karnauskas R, Harris MH, Plas DR, Zhuang H, Cinalli RM, Alavi A, Rudin CM, Thompson CB. Cancer Res. 2004 Jun 1;64(11):3892-9.
19)	Glutamine-driven oxidative phosphorylation is a major ATP source in transformed mammalian cells in both normoxia and hypoxia. **Fan J**, Kamphorst JJ, Mathew R, Chung MK, White E, Shlomi T, Rabinowitz JD. Mol Syst Biol. 2013 Dec 3;9:712. doi: 10.1038/msb.2013.65.
20)	Enzymatic activity associated with class II HDACs is dependent on a multiprotein complex containing HDAC3 and SMRT/N-CoR. **Fischle W**, Dequiedt F, Hendzel MJ, Guenther MG, Lazar MA, Voelter W, Verdin E. Mol Cell. 2002 Jan;9(1):45-57.
21)	The Isopeptidase Inhibitor G5 Triggers a Caspase-independent Necrotic Death in Cells Resistant to Apoptosis: A COMPARATIVE STUDY WITH THE PROTEASOME INHIBITOR BORTEZOMIB. **Fontanini A**, Foti C, Potu H, Crivellato E, Maestro R, Bernardi P, Demarchi F, Brancolini C. J Biol Chem. 2009 Mar 27;284(13):8369-81. doi: 10.1074/jbc.M806113200. Epub 2009 Jan 12.
22)	Glutamine deprivation induces abortive s-phase rescued by deoxyribonucleotides in k-ras transformed fibroblasts. **Gaglio D**, Soldati C, Vanoni M, Alberghina L, Chiaradonna F. PLoS One. 2009;4(3):e4715. doi: 10.1371/journal.pone.0004715. Epub 2009 Mar 5.
23)	Inactivation of ATP citrate lyase by Cucurbitacin B: A bioactive compound from cucumber, inhibits prostate cancer growth. **Gao Y**, Islam MS, Tian J, Lui VW, Xiao D. Cancer Lett. 2014 Jul 10;349(1):15-25. doi: 10.1016/j.canlet.2014.03.015. Epub 2014 Mar 29.
24)	Systemic elevation of PTEN induces a tumor-suppressive metabolic state. **Garcia-Cao I**, Song MS, Hobbs RM, Laurent G, Giorgi C, de Boer VC, Anastasiou D, Ito K, Sasaki AT, Rameh L, Carracedo A, Vander Heiden MG, Cantley LC, Pinton P, Haigis MC, Pandolfi PP. Cell. 2012 Mar 30;149(1):49-62. doi: 10.1016/j.cell.2012.02.030. Epub 2012 Mar 6.
25)	HDAC4 protein regulates HIF1α protein lysine acetylation and cancer cell response to hypoxia. **Geng H**, Harvey CT, Pittsenbarger J, Liu Q, Beer TM, Xue C, Qian DZ. J Biol Chem. 2011 Nov 4;286(44):38095-102. doi: 10.1074/jbc.M111.257055. Epub 2011 Sep 14.
26)	Regulation of histone deacetylase 4 and 5 and transcriptional activity by 14-3-3-dependent cellular localization. **Grozinger CM**, **Schreiber SL**. Proc Natl Acad Sci U S A. 2000 Jul 5;97(14):7835-40.
27)	The hallmarks of cancer. **Hanahan D**, **Weinberg RA**. Cell. 2000 Jan 7;100(1):57-70. Review.
28)	Hallmarks of cancer: the next generation. **Hanahan D**, **Weinberg RA**. Cell. 2011 Mar 4;144(5):646-74. doi: 10.1016/j.cell.2011.02.013. Review.
29)	AMPK--sensing energy while talking to other signaling pathways.

	Hardie DG. Cell Metab. 2014 Dec 2;20(6):939-52. doi: 10.1016/j.cmet.2014.09.013. Epub 2014 Oct 30.
30)	Glutamine and cancer: cell biology, physiology, and clinical opportunities. **Hensley CT**, Wasti AT, DeBerardinis RJ. J Clin Invest. **2013** Sep 3;123(9):3678-84. doi: 10.1172/JCI69600. Epub 2013 Sep 3. Review.
31)	Cancer cell metabolism: Warburg and beyond. **Hsu PP**, **Sabatini DM**. Cell. 2008 Sep 5;134(5):703-7. doi: 10.1016/j.cell.2008.08.021.
32)	Heterogeneity of tumor-induced gene expression changes in the human metabolic network. **Hu J**, Locasale JW, Bielas JH, O'Sullivan J, Sheahan K, Cantley LC, Vander Heiden MG, Vitkup D. Nat Biotechnol. 2013 Jun;31(6):522-9. doi: 10.1038/nbt.2530. Epub 2013 Apr 21.
33)	K-ras(G12V) transformation leads to mitochondrial dysfunction and a metabolic switch from oxidative phosphorylation to glycolysis. **Hu Y**, Lu W, Chen G, Wang P, Chen Z, Zhou Y, Ogasawara M, Trachootham D, Feng L, Pelicano H, Chiao PJ, Keating MJ, Garcia-Manero G, Huang P. Cell Res. 2012 Feb;22(2):399-412. doi: 10.1038/cr.2011.145. Epub 2011 Aug 30.
34)	Acetylation control of metabolic enzymes in cancer: an updated version. **Huang W**, Wang Z, Lei QY. Acta Biochim Biophys Sin (Shanghai). 2014 Mar;46(3):204-13. doi: 10.1093/abbs/gmt154. Epub 2014 Jan 30. Review.
35)	Understanding the central role of citrate in the metabolism of cancer cells. **Icard P**, Poulain L, Lincet H. Biochim Biophys Acta. 2012 Jan;1825(1):111-6. doi: 10.1016/j.bbcan.2011.10.007. Epub 2011 Nov 10. Review.
36)	Repression of sestrin family genes contributes to oncogenic Ras-induced reactive oxygen species up-regulation and genetic instability. **Kopnin PB**, Agapova LS, Kopnin BP, Chumakov PM. Cancer Res. 2007 May 15;67(10):4671-8.
37)	Tumor cell metabolism: cancer's Achilles' heel. **Kroemer G**, **Pouyssegur J**. Cancer Cell. 2008 Jun;13(6):472-82. doi: 10.1016/j.ccr.2008.05.005. Review.
38)	Unraveling the hidden catalytic activity of vertebrate class IIa histone deacetylases. **Lahm A**, Paolini C, Pallaoro M, Nardi MC, Jones P, Neddermann P, Sambucini S, Bottomley MJ, Lo Surdo P, Carfí A, Koch U, De Francesco R, Steinkühler C, Gallinari P. Proc Natl Acad Sci U S A. 2007 Oct 30;104(44):17335-40. Epub 2007 Oct 23.
39)	Inhibition of lactate dehydrogenase A induces oxidative stress and inhibits tumor progression. **Le A**, Cooper CR, Gouw AM, Dinavahi R, Maitra A, Deck LM, Royer RE, Vander Jagt DL, Semenza GL, Dang CV. Proc Natl Acad Sci U S A. 2010 Feb 2;107(5):2037-42. doi: 10.1073/pnas.0914433107. Epub 2010 Jan 19.
40)	The control of the metabolic switch in cancers by oncogenes and tumor suppressor genes. **Levine AJ**, **Puzio-Kuter AM**. Science. 2010 Dec 3;330(6009):1340-4. doi: 10.1126/science.1193494. Review. Erratum in: Science. 2012 May 11;336(6082):670.
41)	Targeting mitochondrial oxidative metabolism in melanoma causes metabolic compensation through glucose and glutamine utilization. **Lim JH**, Luo C, Vazquez F, Puigserver P. Cancer Res. 2014 Jul 1;74(13):3535-45. doi: 10.1158/0008-5472.CAN-13-2893-T. Epub 2014 May 8.
42)	Signal-dependent activation of the MEF2 transcription factor by dissociation from histone deacetylases. **Lu J**, McKinsey TA, Nicol RL, Olson EN. Proc Natl Acad Sci U S A. 2000 Apr 11;97(8):4070-5.
43)	Acetylation targets the M2 isoform of pyruvate kinase for degradation through chaperone-mediated autophagy and promotes tumor growth. **Lv L**, Li D, Zhao D, Lin R, Chu Y, Zhang H, Zha Z, Liu Y, Li Z, Xu Y, Wang G, Huang Y, Xiong Y, Guan KL, Lei QY. Mol Cell. 2011 Jun 24;42(6):719-30. doi: 10.1016/j.molcel.2011.04.025.
44)	Molecular mechanisms of mTOR-mediated translational control. **Ma XM**, **Blenis J**.

	Nat Rev Mol Cell Biol. 2009 May;10(5):307-18. doi: 10.1038/nrm2672. Epub 2009 Apr 2. Review.
45)	mTOR complex 2 controls glycolytic metabolism in glioblastoma through FoxO acetylation and upregulation of c-Myc. **Masui K**, Tanaka K, Akhavan D, Babic I, Gini B, Matsutani T, Iwanami A, Liu F, Villa GR, Gu Y, Campos C, Zhu S, Yang H, Yong WH, Cloughesy TF, Mellinghoff IK, Cavenee WK, Shaw RJ, Mischel PS. Cell Metab. 2013 Nov 5;18(5):726-39. doi: 10.1016/j.cmet.2013.09.013. Epub 2013 Oct 17.
46)	AMP-activated protein kinase regulates GLUT4 transcription by phosphorylating histone deacetylase 5. **McGee SL**, van Denderen BJ, Howlett KF, Mollica J, Schertzer JD, Kemp BE, Hargreaves M. Diabetes. 2008 Apr;57(4):860-7. doi: 10.2337/db07-0843. Epub 2008 Jan 9.
47)	Activation of the myocyte enhancer factor-2 transcription factor by calcium/calmodulin-dependent protein kinase-stimulated binding of 14-3-3 to histone deacetylase 5. **McKinsey TA**, Zhang CL, Olson EN. Proc Natl Acad Sci U S A. 2000 Dec 19;97(26):14400-5.
48)	Fatty acid synthase and the lipogenic phenotype in cancer pathogenesis. **Menendez JA**, Lupu R. Nat Rev Cancer. 2007 Oct;7(10):763-77. Review.
49)	Class IIa histone deacetylases are hormone-activated regulators of FOXO and mammalian glucose homeostasis. **Mihaylova MM**, Vasquez DS, Ravnskjaer K, Denechaud PD, Yu RT, Alvarez JG, Downes M, Evans RM, Montminy M, Shaw RJ. Cell. 2011 May 13;145(4):607-21. doi: 10.1016/j.cell.2011.03.043.
50)	Energy metabolism in tumor cells. Moreno-Sánchez R, Rodríguez-Enríquez S, Marín-Hernández A, Saavedra E. FEBS J. 2007 Mar;274(6):1393-418. Review.
51)	mTORC1 controls mitochondrial activity and biogenesis through 4E-BP-dependent translational regulation. **Morita M**, Gravel SP, Chénard V, Sikström K, Zheng L, Alain T, Gandin V, Avizonis D, Arguello M, Zakaria C, McLaughlan S, Nouet Y, Pause A, Pollak M, Gottlieb E, Larsson O, St-Pierre J, Topisirovic I, Sonenberg N. Cell Metab. 2013 Nov 5;18(5):698-711. doi: 10.1016/j.cmet.2013.10.001.
52)	HDAC4 represses p21(WAF1/Cip1) expression in human cancer cells through a Sp1-dependent, p53-independent mechanism. **Mottet D**, Pirotte S, Lamour V, Hagedorn M, Javerzat S, Bikfalvi A, Bellahcène A, Verdin E, Castronovo V. Oncogene. 2009 Jan 15;28(2):243-56. doi: 10.1038/onc.2008.371. Epub 2008 Oct 13.
53)	Cooperation between complexes that regulate chromatin structure and transcription. **Narlikar GJ**, Fan HY, Kingston RE. Cell. 2002 Feb 22;108(4):475-87. Review.
54)	The role of CaMKII in regulating GLUT4 expression in skeletal muscle. **Ojuka EO**, Goyaram V, Smith JA. Am J Physiol Endocrinol Metab. 2012 Aug 1;303(3):E322-31. doi: 10.1152/ajpendo.00091.2012. Epub 2012 Apr 10. Review.
55)	Oncogenic K-ras expression is associated with derangement of the cAMP/PKA pathway and forskolin-reversible alterations of mitochondrial dynamics and respiration. **Palorini R**, De Rasmo D, Gaviraghi M, Sala Danna L, Signorile A, Cirulli C, Chiaradonna F, Alberghina L, Papa S. Oncogene. 2013 Jan 17;32(3):352-62. doi: 10.1038/onc.2012.50. Epub 2012 Mar 12.
56)	Caspase-dependent regulation of histone deacetylase 4 nuclear-cytoplasmic shuttling promotes apoptosis. **Paroni G**, Mizzau M, Henderson C, Del Sal G, Schneider C, Brancolini C. Mol Biol Cell. 2004 Jun;15(6):2804-18. Epub 2004 Apr 9.
57)	Histone deacetylase degradation and MEF2 activation promote the formation of slow-twitch myofibers. **Potthoff MJ**, Wu H, Arnold MA, Shelton JM, Backs J, McAnally J, Richardson JA, Bassel-Duby R, Olson EN. J Clin Invest. 2007 Sep;117(9):2459-67.
58)	Class II histone deacetylases are associated with VHL-independent regulation of hypoxia-inducible factor 1 alpha.

	Qian DZ, Kachhap SK, Collis SJ, Verheul HM, Carducci MA, Atadja P, Pili R. Cancer Res. 2006 Sep 1;66(17):8814-21.
59)	Perturbational profiling of a cell-line model of tumorigenesis by using metabolic measurements. **Ramanathan A**, Wang C, Schreiber SL. Proc Natl Acad Sci U S A. 2005 Apr 26;102(17):5992-7. Epub 2005 Apr 19.
60)	H-Ras-driven tumoral maintenance is sustained through caveolin-1-dependent alterations in calcium signaling. **Rimessi A**, Marchi S, Patergnani S, Pinton P. Oncogene. 2014 May 1;33(18):2329-40. doi: 10.1038/onc.2013.192. Epub 2013 Jun 3.
61)	Blocking anaplerotic entry of glutamine into the TCA cycle sensitizes K-Ras mutant cancer cells to cytotoxic drugs. **Saqcena M**, Mukhopadhyay S, Hosny C, Alhamed A, Chatterjee A, Foster DA. Oncogene. 2014 Jul 14. doi: 10.1038/onc.2014.207. [Epub ahead of print]
62)	Lysine acetylation activates 6-phosphogluconate dehydrogenase to promote tumor growth. **Shan C**, Elf S, Ji Q, Kang HB, Zhou L, Hitosugi T, Jin L, Lin R, Zhang L, Seo JH, Xie J, Tucker M, Gu TL, Sudderth J, Jiang L, DeBerardinis RJ, Wu S, Li Y, Mao H, Chen PR, Wang D, Chen GZ, Lonial S, Arellano ML, Khoury HJ, Khuri FR, Lee BH, Brat DJ, Ye K, Boggon TJ, He C, Kang S, Fan J, Chen J. Mol Cell. 2014 Aug 21;55(4):552-65. doi: 10.1016/j.molcel.2014.06.020. Epub 2014 Jul 17.
63)	Ras, PI(3)K and mTOR signalling controls tumour cell growth. **Shaw RJ**, **Cantley LC**. Nature. 2006 May 25;441(7092):424-30. Review.
64)	Transcription factor NRF2 regulates miR-1 and miR-206 to drive tumorigenesis. **Singh A**, Happel C, Manna SK, Acquaah-Mensah G, Carrerero J, Kumar S, Nasipuri P, Krausz KW, Wakabayashi N, Dewi R, Boros LG, Gonzalez FJ, Gabrielson E, Wong KK, Girnun G, Biswal S. J Clin Invest. 2013 Jul 1;123(7):2921-34. doi: 10.1172/JCI66353. Epub 2013 Jun 10.
65)	Mammalian target of rapamycin up-regulation of pyruvate kinase isoenzyme type M2 is critical for aerobic glycolysis and tumor growth. **Sun Q**, Chen X, Ma J, Peng H, Wang F, Zha X, Wang Y, Jing Y, Yang H, Chen R, Chang L, Zhang Y, Goto J, Onda H, Chen T, Wang MR, Lu Y, You H, Kwiatkowski D, Zhang H. Proc Natl Acad Sci U S A. 2011 Mar 8;108(10):4129-34. doi: 10.1073/pnas.1014769108. Epub 2011 Feb 15.
66)	How do cancer cells acquire the fuel needed to support cell growth? **Thompson CB**, Bauer DE, Lum JJ, Hatzivassiliou G, Zong WX, Zhao F, Ditsworth D, Buzzai M, Lindsten T. Cold Spring Harb Symp Quant Biol. 2005;70:357-62.
67)	Understanding the Warburg effect: the metabolic requirements of cell proliferation. **Vander Heiden MG**, Cantley LC, Thompson CB. Science. 2009 May 22;324(5930):1029-33. doi: 10.1126/science.1160809. Review.
68)	PGC1α expression defines a subset of human melanoma tumors with increased mitochondrial capacity and resistance to oxidative stress. **Vazquez F**, Lim JH, Chim H, Bhalla K, Girnun G, Pierce K, Clish CB, Granter SR, Widlund HR, Spiegelman BM, Puigserver P. Cancer Cell. 2013 Mar 18;23(3):287-301. Doi: 10.1016/j.ccr.2012.11.020. Epub 2013 Feb 14.
69)	Regulation of histone deacetylase 4 by binding of 14-3-3 proteins. **Wang AH**, Kruhlak MJ, Wu J, Bertos NR, Vezmar M, Posner BI, Bazett-Jones DP, Yang XJ. Mol Cell Biol. 2000 Sep;20(18):6904-12.
70)	Histone deacetylase 4 possesses intrinsic nuclear import and export signals. **Wang AH**, **Yang XJ**. Mol Cell Biol. 2001 Sep;21(17):5992-6005.
71)	A hormone-dependent module regulating energy balance. **Wang B**, Moya N, Niessen S, Hoover H, Mihaylova MM, Shaw RJ, Yates JR 3rd, Fischer WH, Thomas JB, Montminy M. Cell. 2011 May 13;145(4):596-606. doi: 10.1016/j.cell.2011.04.013.
72)	Glycolysis-dependent histone deacetylase 4 degradation regulates inflammatory cytokine production. **Wang B**, Liu TY, Lai CH, Rao YH, Choi MC, Chi JT, Dai JW, Rathmell JC, Yao TP. Mol Biol Cell. 2014 Nov 1;25(21):3300-7. doi: 10.1091/mbc.E13-12-0757. Epub 2014 Sep 3.
73)	Genome-wide mapping of HATs and HDACs reveals distinct functions in active and inactive genes.

	Wang Z, Zang C, Cui K, Schones DE, Barski A, Peng W, Zhao K. Cell. 2009 Sep 4;138(5):1019-31. doi: 10.1016/j.cell.2009.06.049. Epub 2009 Aug 20.
74)	The metabolism of tumors in the body. **Warburg O**, Wind F, Negelein E. J Gen Physiol. 1927 Mar 7;8(6):519-30.
75)	On the origin of cancer cells. **Warburg O**. Science. 1956 Feb 24;123(3191):309-14.
76)	Metabolic reprogramming: a cancer hallmark even warburg did not anticipate. **Ward PS**, **Thompson CB**. Cancer Cell. 2012 Mar 20;21(3):297-308. doi: 10.1016/j.ccr.2012.02.014. Review.
77)	Structure of HDAC3 bound to co-repressor and inositol tetraphosphate. **Watson PJ**, Fairall L, Santos GM, Schwabe JW. Nature. 2012 Jan 9;481(7381):335-40. doi: 10.1038/nature10728.
78)	Class II histone deacetylases downregulate GLUT4 transcription in response to increased cAMP signaling in cultured adipocytes and fasting mice. **Weems JC**, Griesel BA, Olson AL. Diabetes. 2012 Jun;61(6):1404-14. doi: 10.2337/db11-0737. Epub 2012 Mar 8.
79)	miR-181a mediates metabolic shift in colon cancer cells via the PTEN/AKT pathway. **Wei Z**, Cui L, Mei Z, Liu M, Zhang D. FEBS Lett. 2014 May 2;588(9):1773-9. doi: 10.1016/j.febslet.2014.03.037. Epub 2014 Mar 28.
80)	Mitochondrial metabolism and ROS generation are essential for Kras-mediated tumorigenicity. **Weinberg F**, Hamanaka R, Wheaton WW, Weinberg S, Joseph J, Lopez M, Kalyanaraman B, Mutlu GM, Budinger GR, Chandel NS. Proc Natl Acad Sci U S A. 2010 May 11;107(19):8788-93. doi: 10.1073/pnas.1003428107. Epub 2010 Apr 26.
81)	HDAC4 promotes growth of colon cancer cells via repression of p21. **Wilson AJ**, Byun DS, Nasser S, Murray LB, Ayyanar K, Arango D, Figueroa M, Melnick A, Kao GD, Augenlicht LH, Mariadason JM. Mol Biol Cell. 2008 Oct;19(10):4062-75. doi: 10.1091/mbc.E08-02-0139. Epub 2008 Jul 16.
82)	Myc regulates a transcriptional program that stimulates mitochondrial glutaminolysis and leads to glutamine addiction. **Wise DR**, DeBerardinis RJ, Mancuso A, Sayed N, Zhang XY, Pfeiffer HK, Nissim I, Daikhin E, Yudkoff M, McMahon SB, Thompson CB. Proc Natl Acad Sci U S A. 2008 Dec 2;105(48):18782-7. doi: 10.1073/pnas.0810199105. Epub 2008 Nov 24.
83)	Impairment of mitochondrial respiration in mouse fibroblasts by oncogenic H-RAS(Q61L). **Yang D**, Wang MT, Tang Y, Chen Y, Jiang H, Jones TT, Rao K, Brewer GJ, Singh KK, Nie D. Cancer Biol Ther. 2010 Jan;9(2):122-33. Epub 2010 Jan 21.
84)	Identification of HDAC4 as a target of γ-catenin that regulates the oncogenic K-Ras-mediated malignant phenotype of Rat2 cells. **Yim JH**, Baek JH, Lee CW, Kim MJ, Yun HS, Hong EH, Lee SJ, Park JK, Um HD, Hwang SG. Biochem Biophys Res Commun. 2013 Jul 5;436(3):436-42. doi: 10.1016/j.bbrc.2013.05.122. Epub 2013 Jun 6.
85)	2-Deoxy-D-glucose targeting of glucose metabolism in cancer cells as a potential therapy. **Zhang D**, Li J, Wang F, Hu J, Wang S, Sun Y. Cancer Lett. 2014 Dec 28;355(2):176-83. doi: 10.1016/j.canlet.2014.09.003. Epub 2014 Sep 10.
86)	Histone deacetylase 4 associates with extracellular signal-regulated kinases 1 and 2, and its cellular localization is regulated by oncogenic Ras. **Zhou X**, Richon VM, Wang AH, Yang XJ, Rifkind RA, Marks PA. Proc Natl Acad Sci U S A. 2000 Dec 19;97(26):14329-33.
87)	Cloning and characterization of a histone deacetylase, HDAC9. **Zhou X**, Marks PA, Rifkind RA, Richon VM. Proc Natl Acad Sci U S A. 2001 Sep 11;98(19):10572-7. Epub 2001 Sep 4.
88)	mTOR: from growth signal integration to cancer, diabetes and ageing. **Zoncu R**, Efeyan A, Sabatini DM. Nat Rev Mol Cell Biol. 2011 Jan;12(1):21-35. doi: 10.1038/nrm3025. Epub 2010 Dec 15. Review.

ACKNOWLEDGEMENTS

First of all, I want to thank all my dearest Lab Friends. I can't imagine my Doctoral path without them and their encouraging support. As I wrote elsewhere, the most important people that one meet during the life are kept in the heart forever. I don't make an exception.

My sweetest gratefulness goes to my family, Jusy Nikola and Maki, whose sympathetic smiles and unconditioned tenderness always make me feel as if no unsolvable problem exists.

Finally, I need to express my gratitude to Prof. Irene Mavelli and Prof. Claudio Brancolini for their availability, care and precious help in reviewing this thesis and for their suggestions during my entire PhD.